

AD 737839

INVESTIGATION OF THE ABSORPTION OF  
INFRARED RADIATION BY NITROUS OXIDE  
FROM 760 to 2380  $\text{cm}^{-1}$   
(13.2 to 4.2  $\mu\text{m}$ )

by

Darrell E. Burch  
David A. Gryvnak  
John D. Pembroke

Philco-Ford Corporation  
Aeronutronic Division  
Ford Road  
Newport Beach, California 92663

Contract No. F19628-69-C-0263  
Project No. 5130

Semi-Annual Technical Report No. 4

December 1971

The views and conclusions contained in this document are those of the authors and should not be interpreted as necessarily representing the official policies, either expressed or implied, of the Advanced Research Projects Agency, or the U. S. Government.

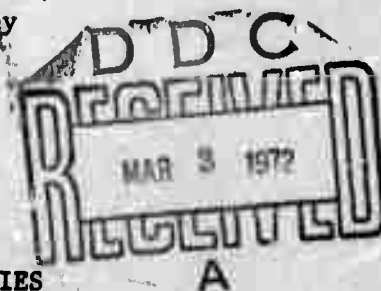
Approved for public release; distribution unlimited.

Contract Monitor: Robert A. McClatchey  
Optical Physics Laboratory

Sponsored by  
Advanced Research Projects Agency  
ARPA Order No. 1366

Monitored by  
AIR FORCE CAMBRIDGE RESEARCH LABORATORIES  
AIR FORCE SYSTEMS COMMAND  
UNITED STATES AIR FORCE  
BEDFORD, MASSACHUSETTS 01730

Reproduced by  
NATIONAL TECHNICAL  
INFORMATION SERVICE  
Springfield, Va. 22151



RHS



## DOCUMENT CONTROL DATA - R &amp; D

(Security classification of title, body of abstract and indexing annotation must be entered when the overall report is classified)

## 1. ORIGINATING ACTIVITY (Corporate author)

Philco-Ford Corporation  
Aeronutronic Division  
Newport Beach, California 92663

## 2a. REPORT SECURITY CLASSIFICATION

Unclassified

## 2b. GROUP

## 3. REPORT TITLE

INVESTIGATION OF THE ABSORPTION OF INFRARED RADIATION BY NITROUS OXIDE FROM  
760 TO 2380  $\text{cm}^{-1}$  (13.1 TO 4.2  $\mu\text{m}$ )

## 4. DESCRIPTIVE NOTES (Type of report and inclusive dates)

Scientific Interim

## 5. AUTHOR(S) (First name, middle initial, last name)

Darrell E. Burch  
David A. Gryvnak  
John D. Pembroke

## 6. REPORT DATE

December 1971

## 7a. TOTAL NO. OF PAGES

43

## 7b. NO. OF REFS

7

## 8a. CONTRACT OR GRANT NO.

FL9628-69-C-0263 ARPA Order No. 1366  
b. PROJECT NO. 5130

## 9a. ORIGINATOR'S REPORT NUMBER(S)

U-4995  
Semi-Annual Technical Report No. 4

## 9b. OTHER REPORT NO(S) (Any other numbers that may be assigned this report)

AFCRL-71-0620

c. DOD Element 62301D

d. DOD Supplement n/a

## 10. DISTRIBUTION STATEMENT

A-Approved for public release; distribution unlimited.

## 11. SUPPLEMENTARY NOTES

Tech, Other

## 12. SPONSORING MILITARY ACTIVITY

Air Force Cambridge Research Laboratories(OR)  
L. G. Hanscom Field  
Bedford, Massachusetts 01730

## 13. ABSTRACT

Experimental data are presented on the absorption by a variety of  $\text{N}_2\text{O}$  samples between 760 and 2380  $\text{cm}^{-1}$ . Most of the absorption between 760 and 850  $\text{cm}^{-1}$  is due to extreme wings of lines centered outside the interval. Strengths of the important band systems are given. Curves of transmittance and tables of integrated absorptance and the integrated absorption coefficient provide detailed information on the absorption. The objective of the study is to provide the data required to determine the parameters of all  $\text{N}_2\text{O}$  absorption lines that absorb significantly over any atmospheric path of interest.

14.

## KEY WORDS

## LINK A

## LINK B

## LINK C

ROLE

WT

ROLE

WT

ROLE

WT

 $N_2O$ 

Atmospheric Transmission

Absorption

INVESTIGATION OF THE ABSORPTION OF  
INFRARED RADIATION BY NITROUS OXIDE  
FROM 760 to 2380  $\text{cm}^{-1}$   
(13.2 to 4.2  $\mu\text{m}$ )

by

Darrell E. Burch  
David A. Gryvnak  
John D. Pembroke

Philco-Ford Corporation  
Aeronutronic Division  
Ford Road  
Newport Beach, California 92663

Contract No. F19628-69-C-0263  
Project No. 5130

Semi-Annual Technical Report No. 4

December 1971

The views and conclusions contained in this document are those of the authors and should not be interpreted as necessarily representing the official policies, either expressed or implied, of the Advanced Research Projects Agency, or the U. S. Government.

Approved for public release; distribution unlimited.

Contract Monitor: Robert A. McClatchey  
Optical Physics Laboratory

Sponsored by  
Advanced Research Projects Agency  
ARPA Order No. 1366  
Monitored by  
AIR FORCE CAMBRIDGE RESEARCH LABORATORIES  
AIR FORCE SYSTEMS COMMAND  
UNITED STATES AIR FORCE  
BEDFORD, MASSACHUSETTS 01730

INVESTIGATION OF THE ABSORPTION OF  
INFRARED RADIATION BY NITROUS OXIDE  
FROM 760 to 2380  $\text{cm}^{-1}$   
(13.2 to 4.2  $\mu\text{m}$ )

by

Darrell E. Burch  
David A. Gryvnak  
John D. Pembroke

Philco-Ford Corporation  
Aeronutronic Division  
Ford Road  
Newport Beach, California 92663

Contract No. F19628-69-C-0263  
Project No. 5130

Semi-Annual Technical Report No. 4

December 1971

The views and conclusions contained in this document are those of the authors and should not be interpreted as necessarily representing the official policies, either expressed or implied, of the Advanced Research Projects Agency, or the U. S. Government.

Approved for public release; distribution unlimited.

Contract Monitor: Robert A. McClatchey  
Optical Physics Laboratory

Sponsored by  
Advanced Research Projects Agency  
ARPA Order No. 1366  
Monitored by  
AIR FORCE CAMBRIDGE RESEARCH LABORATORIES  
AIR FORCE SYSTEMS COMMAND  
UNITED STATES AIR FORCE  
BEDFORD, MASSACHUSETTS 01730

# ABSTRACT

Experimental data are presented on the absorption by a variety of  $\text{N}_2\text{O}$  samples between 760 and 2380  $\text{cm}^{-1}$ . Most of the absorption between 760 and 850  $\text{cm}^{-1}$  is due to extreme wings of lines centered outside the interval. Strengths of the important band systems are given. Curves of transmittance and tables of integrated absorptance and the integrated absorption coefficient provide detailed information on the absorption. The objective of the study is to provide the data required to determine the parameters of all  $\text{N}_2\text{O}$  absorption lines that absorb significantly over any atmospheric path of interest.

## TABLE OF CONTENTS

SECTION	PAGE
1 INTRODUCTION AND SUMMARY . . . . .	1-1
2 ABSORPTION BETWEEN 760 AND 1100 $\text{cm}^{-1}$ . . . . .	2-1
Figure 2-1. Spectral curve of the normalized absorption absorption coefficient for continuum absorption by pure $\text{N}_2\text{O}$ at 296°K . . . . .	2-2
Figure 2-2. Spectral curve of transmittance from 850 to 1100 $\text{cm}^{-1}$ . . . . .	2-3
Figure 2-3. Spectral curve of $(-1/u) \ln T$ from 850 to 1100 $\text{cm}^{-1}$ . . . . .	2-4
Table 2-1. Integrated Absorption Coefficient between 845 and 1105 $\text{cm}^{-1}$ . . . . .	2-5
Figure 2-4. Spectral curve of absorptance from 905 to 960 $\text{cm}^{-1}$ . . . . .	2-7
Figure 2-5. Spectral curve of absorptance from 860 to 905 $\text{cm}^{-1}$ and from 961 to 1000 $\text{cm}^{-1}$ . . . . .	2-8
3 ABSORPTION BETWEEN 1100 AND 1350 $\text{cm}^{-1}$ . . . . .	3-1
Figure 3-1. Spectral curve of transmittance from 1110 to 1250 $\text{cm}^{-1}$ . . . . .	3-3
Figure 3-2. Spectral curve of transmittance from 1220 to 1350 $\text{cm}^{-1}$ . . . . .	3-4
Figure 3-3. Spectral curve of $(-1/u) \ln T$ for $\text{N}_2\text{O}$ from 1110 to 1250 $\text{cm}^{-1}$ . . . . .	3-5



# TABLE OF CONTENTS (Continued)

SECTION	PAGE
Figure 3-4. Spectral curve of $(-1/u) \ln T$ for $N_2O$ from 1220 to 1350 $cm^{-1}$ . . . . .	3-6
Table 3-1. Integrated Absorption Coefficient between 1110 and 1335 $cm^{-1}$ . . . . .	3-7
Figure 3-5. Spectral curve of transmittance from 1115 to 1215 $cm^{-1}$ . . . . .	3-8
Figure 3-6. Spectral curve of transmittance from 1115 to 1230 $cm^{-1}$ . . . . .	3-9
Figure 3-7. Spectral curve of transmittance from 1115 to 1215 $cm^{-1}$ . . . . .	3-10
Table 3-2. $[\int_{\nu'}^{\nu} A(\nu) d\nu]$ ( $\nu'=1115 \text{ } cm^{-1}$ ) . . . . .	3-11
Figure 3-8. Spectral curve of transmittance from 1200 to 1335 $cm^{-1}$ . . . . .	3-12
Figure 3-9. Spectral curve of transmittance from 1240 to 1335 $cm^{-1}$ . . . . .	3-13
Figure 3-10. Spectral curve of transmittance from 1240 to 1335 $cm^{-1}$ . . . . .	3-14
Table 3-3. $[\int_{\nu'}^{\nu} A(\nu) d\nu]$ ( $\nu'=1240 \text{ } cm^{-1}$ ) . . . . .	3-15
4 ABSORPTION BETWEEN 2100 AND 2380 $cm^{-1}$ . . . . .	4-1
Figure 4-1. Spectral curve of transmittance from 2100 to 2380 $cm^{-1}$ for several samples at pressures greater than 7 atm . . . . .	4-3
Figure 4-2. Spectral curves of $(-1/u) \ln T$ between 2140 and 2280 $cm^{-1}$ . . . . .	4-4
Table 4-1. Sample Parameters . . . . .	4-5
Table 4-2. Integrated absorption coefficient between 2145 and 2280 $cm^{-1}$ . . . . .	4-6
Table 4-3. $[\int_{\nu'}^{\nu} A(\nu) d\nu]$ ( $\nu'=2162 \text{ } cm^{-1}$ ) . . . . .	4-7

# TABLE OF CONTENTS (Continued)

SECTION	PAGE
Figure 4-3. Spectral curves of transmittance between 2165 and 2210 $\text{cm}^{-1}$ . . . . .	4-8
Figure 4-4. Spectral curves of transmittance between 2210 and 2260 $\text{cm}^{-1}$ . . . . .	4-9
Figure 4-5. Spectral curves of transmittance for a sample at $0.87 \times 10^{-4}$ atm. . . . .	4-10
5 REFERENCES . . . . .	5-1

## SECTION 1

### INTRODUCTION AND SUMMARY

The work reported herein is part of a large program devoted to the determination and listing of the parameters of all of the spectral lines that absorb significantly in the earth's atmosphere. When completed, the listing will include the parameters such as center position, normalized half-width, strength, and the lower energy level for each line. From this information, the molecular absorption can be calculated for virtually any atmospheric path of interest. Nitrous oxide is included in this study, since it is a permanent constituent of the atmosphere. Generally,  $\text{N}_2\text{O}$  lines weaker than  $4 \times 10^{-23} \text{ molecules}^{-1} \text{cm}^2 \text{cm}^{-1}$  are not considered significant in applications to the earth's atmosphere and will not be included in the listing. A few of the spectral curves shown in this report include lines weaker than this cut-off value because stronger lines in the same region are above the cut-off. The curves may also be useful to workers interested in larger  $\text{N}_2\text{O}$  samples than are encountered in atmospheric studies. A few lines weaker than the cut-off value may be included in the listing if they belong to a Q-branch which consists of many closely-spaced lines. In these places, the combination of lines may contribute significantly, although any one of them is very weak.

Measuring the parameters of each individual absorption line would be an impossible task. Many of the lines overlap each other and are too close to be resolved by spectrometers with finite resolving power. The parameters are being determined by a combination of experiment and theory. The strength of a band system is determined experimentally from spectral curves similar to some shown in this report. The band system typically consists of a main band as well as some associated difference bands that arise from transitions from excited energy levels with the same changes in the vibrational quantum numbers as the main band. Corresponding bands of the rare isotopic molecules also overlap the main band. In many cases,

the vibration-rotation interaction does not influence the line strengths significantly and the strength of an individual line can be calculated accurately from the strength of the entire vibration band to which it belongs. The relative strengths of the lines within a band have been tabulated by Young<sup>1</sup> for several types of bands.

The relative strengths of the bands within a system can frequently be estimated on the basis of the relative populations of the lower energy levels involved in the transition. Thus, in many cases, the strengths of the individual lines can be calculated from the experimentally-determined strength of the band system. However, the relative strengths of many of the bands can not be predicted by the simple theory. A considerable portion of the present study has been devoted to investigations of the relative strengths of  $\Sigma \leftarrow \Sigma$  bands and their associated difference bands of the  $\Pi \leftarrow \Pi$  type. Experimental spectral curves of transmittance are compared with corresponding curves computed on the basis of the calculated line parameters. From these comparisons, it is possible to determine if the calculated strength of a line is too high or too low. This phase of the study has not yet been completed and none of the results are presented in this report.

Sections 2, 3, and 4 include experimental results on absorption by  $N_2O$  from 760 to 2380  $cm^{-1}$ . No data are included in the 1350 to 2100  $cm^{-1}$  region which does not contain any strong bands. The band system that includes the  $11^10 \leftarrow 00^00$  band centered near 1880  $cm^{-1}$  has a strength of  $1.66 \times 10^{-20}$  ( $\pm 5\%$ ) molecules $^{-1}cm^2cm^{-1}$ . Several of the lines of this band are strong enough to be included in the listing. Eggers and Crawford<sup>2</sup> observed a strength of  $1.53 \times 10^{-20}$  molecules $^{-1}cm^2cm^{-1}$  for this band system. Their value is approximately 8% less than ours. The  $20^00 \leftarrow 01^10$  band centered near 1974  $cm^{-1}$  contains a Q-branch whose strength is  $2.4 \times 10^{-22}$  molecules $^{-1}cm^2cm^{-1}$ . Further work is planned before the detailed results on the 1350 to 2100  $cm^{-1}$  region will be reported.

The data presented in Sections 2, 3, and 4 are intended for use in determining the strengths of the various band systems and for comparison with computer data based on the observed band strengths and theory. The data are presented as spectral curves for a variety of samples and as tables of the integrated absorptance and integrated absorption coefficient. The experimental procedures have been discussed previously<sup>3</sup>. Unless they are indicated otherwise, the positions of band centers and line centers are based on two articles by Pliva<sup>4,5</sup>.

## SECTION 2

### ABSORPTION BETWEEN 760 AND 1100 $\text{cm}^{-1}$

Spectral scans were made throughout the 760 to 850  $\text{cm}^{-1}$  region for a variety of large samples of pure  $\text{N}_2\text{O}$ , including one with  $L = 931$  m and  $p = 1$  atm. No structure was observed other than some near 775  $\text{cm}^{-1}$  that was attributed to a trace of  $\text{NO}_2$  impurity in the  $\text{N}_2\text{O}$ . We concluded that no intrinsic  $\text{N}_2\text{O}$  bands occur in this region with strengths greater than  $10^{-24}$  molecules $^{-1}\text{cm}^2\text{cm}^{-1}$ . Near 750  $\text{cm}^{-1}$ , a few lines were observed and attributed to the wing of the  $10^{00} \leftarrow 01^{10}$  system centered near 696  $\text{cm}^{-1}$ .

Although no line structure was observed, the samples produced significant continuum absorption which may be attributed to the extreme wings of the lines centered outside the interval. The absorption coefficient of the extreme wing of a collision-broadened absorption line increases linearly with pressure, as does the absorber thickness  $u$  for a sample cell of fixed length. Thus  $(-\ln T)$  for continuum absorption is proportional to  $p^2L$ .

By investigating a series of pure  $\text{N}_2\text{O}$  samples covering a range of pressures and path lengths, we determined the normalized absorption coefficient for continuum absorption throughout this spectral region. The results are shown in Fig. 2-1. The transmittance due to continuum for pure  $\text{N}_2\text{O}$  can be calculated from values taken from Fig. 2-1 by:

$$-\ln T = C_s^0 u p,$$

where the subscript (s) denotes self-broadening,  $u$  is the absorber thickness (in molecules  $\text{cm}^{-2}$ ) and  $p$  is the pressure in atm. The increase in the coefficient with decreasing wavenumber from the minimum near 830  $\text{cm}^{-1}$  can be explained in terms of the lines of the 696  $\text{cm}^{-1}$  band. The contribution of each line increases as its center is approached. Similarly, the increase between 830 and 850  $\text{cm}^{-1}$  is probably due to the lines in the

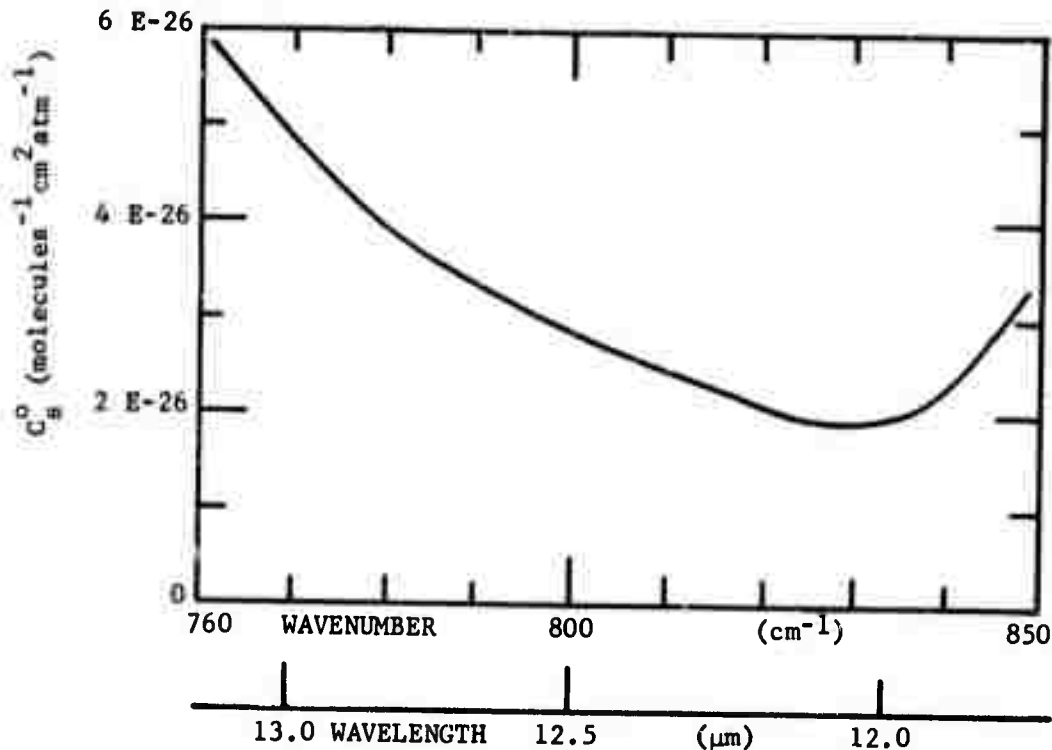


FIG. 2-1. Spectral curve of the normalized absorption coefficient for continuum absorption by pure  $N_2O$  at  $296^\circ K$ .

$00^0_1 \leftarrow 10^0_0$  band centered near  $939\text{ cm}^{-1}$ . In the ordinate of Fig. 2-1 and other similar figures,  $2\text{ E-26}$  denotes  $2 \times 10^{-26}$ , etc.

Most of the absorption between  $850$  and  $1100\text{ cm}^{-1}$  is due to the two "cross-over" bands,  $00^0_1 \leftarrow 02^0_0$  and  $00^0_1 \leftarrow 10^0_0$ , centered at  $1055.622$  and  $938.849\text{ cm}^{-1}$ , respectively. The associated difference bands arising from transitions from higher excited levels are also present. Figure 2-2 shows a spectral curve of transmittance for a sample at sufficiently high pressure that much of the line structure is smoothed out. The remaining line structure is smoothed by the finite slitwidth of the spectrometer. The P and R branches of the two bands are apparent. Figure 2-3 shows the corresponding spectral curve of  $(-1/u) \ln T$ . This quantity is nearly independent of  $u$  and pressure for pressures sufficiently high that the line structure is smoothed out.

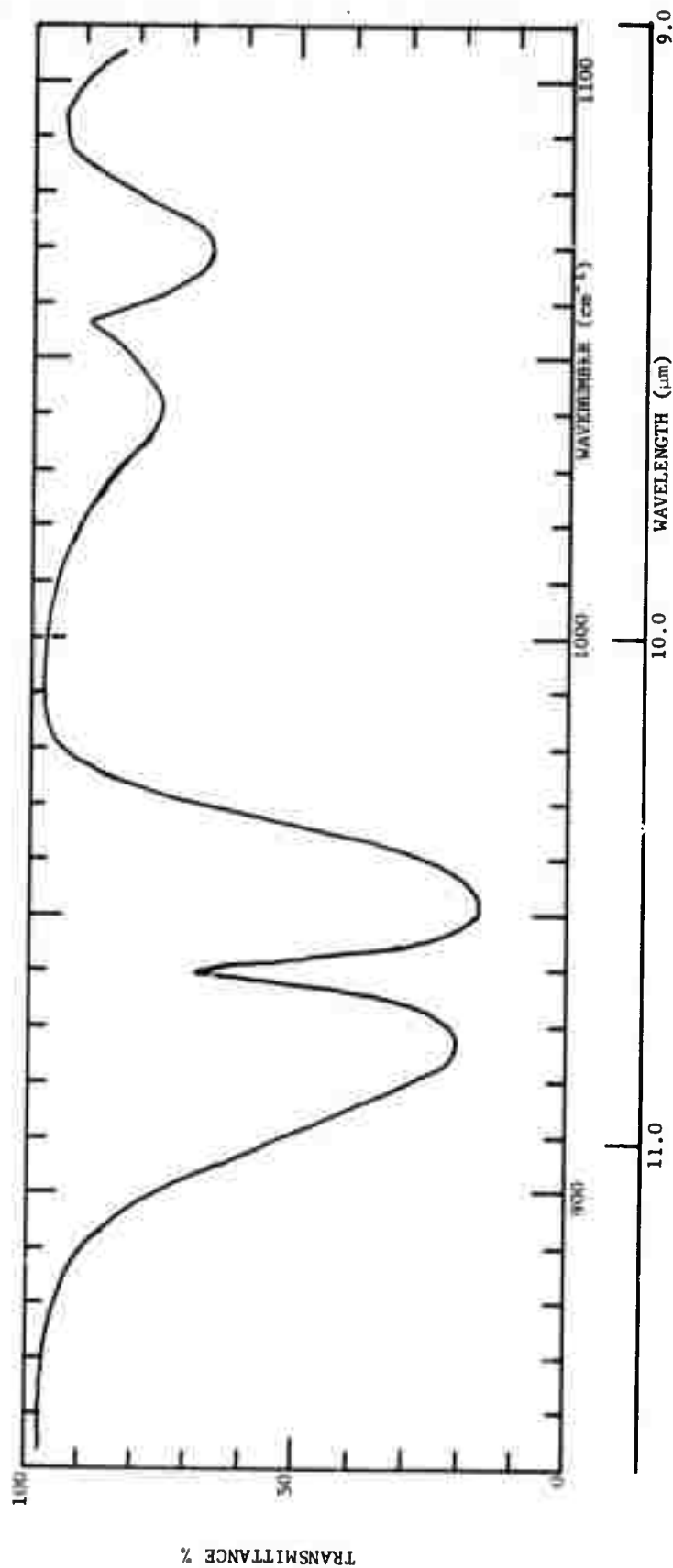


FIG. 2-2. Spectral curve of transmittance from 850 to 1100  $\text{cm}^{-1}$ . The sample was 3.04 atm of pure  $\text{N}_2\text{O}$  at 296 K.  $L = 4.16$  m;  $u = 319 \times 10^{20}$  molecules/ $\text{cm}^2$ . Spectral slitwidth is approximately  $1.2 \text{ cm}^{-1}$ .

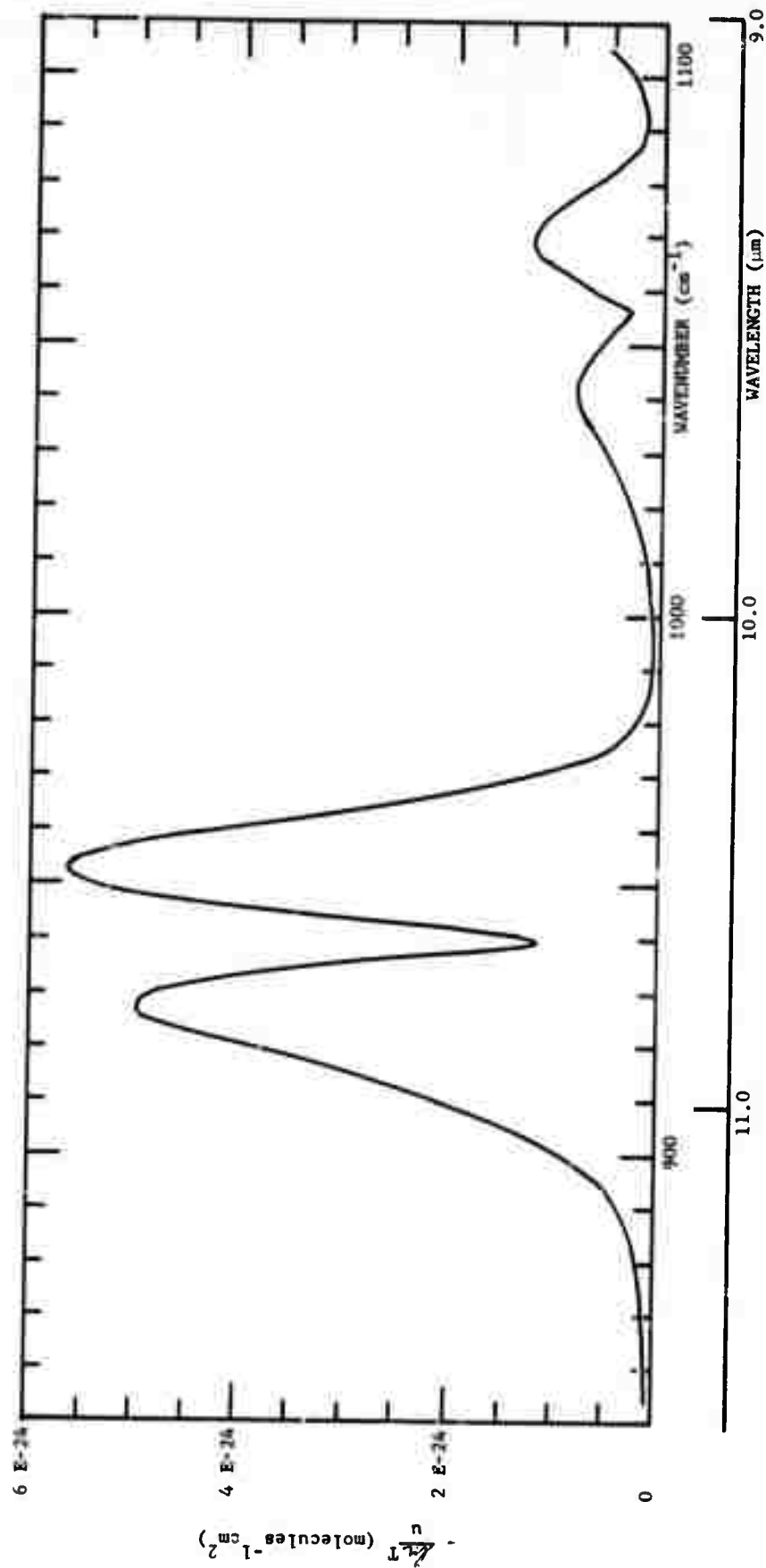


FIG. 2-3. Spectral curve of  $(-1/u) \frac{dT}{dT}$  from 850 to 1100  $\text{cm}^{-1}$ . The curve is based on the sample represented in Fig. 2-1.



TABLE 2-1

INTEGRATED ABSORPTION COEFFICIENT BETWEEN 845 AND 1105  $\text{cm}^{-1}$ 

$$\frac{1}{u} \int_{845}^{\nu} (-\ln T) d\nu$$

(Multiply all values by  $10^{-24}$  molecules $^{-1}$ cm $^2$ cm $^{-1}$ )

$\nu$ ( $\text{cm}^{-1}$ )		$\nu$ ( $\text{cm}^{-1}$ )	
850	3.2	990	2530.1
860	10.1	1000	2537.4
870	18.2	1010	2548.2
880	31.9	1020	2569.1
890	56.1	1030	2610.6
900	114.2	1040	2682.9
910	257.5	1050	2760.9
920	548.3	1056 <sup>c</sup>	2790.9
930	1017.3	1060	2810.3
939 <sup>c</sup>	1311.8	1070	2919.3
940	1323.9	1080	3021.9
950	1687.7	1090	3058.0
960	2208.1	1100	3080.1
970	2465.1	1105	3100.8
980	2519.6		

<sup>c</sup> Denotes position near center of one of the stronger bands.

Table 2-1 gives values of the cumulative integral of the absorption coefficient. The lower limit of integration is  $845 \text{ cm}^{-1}$ . By assuming that the absorption from  $845$  to  $1000 \text{ cm}^{-1}$  is due to the  $00^01 \leftarrow 10^00$  band and its associated difference bands, and that from  $1000$  to  $1100 \text{ cm}^{-1}$  is due to the  $00^01 \leftarrow 02^00$  band and its associated bands, we can determine the strengths of each band system from Table 2-1. The tabulated value of  $\int (-1/u) \ln T d\nu$  at  $1000 \text{ cm}^{-1}$  is  $2537.4 \times 10^{-24}$  molecules $^{-1}$ cm $^2$ cm $^{-1}$ ; therefore, the strength of the  $00^01 \leftarrow 10^00$  band system is approximately  $254 \times 10^{-23}$  molecules $^{-1}$ cm $^2$ cm $^{-1}$ . The strength of the  $00^01 \leftarrow 02^00$  band system is approximately  $54 \times 10^{-23}$  molecules $^{-1}$ cm $^2$ cm $^{-1}$ . The estimated uncertainty is  $\pm 4\%$  for the  $00^01 \leftarrow 00^00$  system and  $\pm 8\%$  for the weaker  $00^01 \leftarrow 02^00$  system which is overlapped by the wing of the much stronger  $02^00$  band centered near  $1168 \text{ cm}^{-1}$ .

Similarly, we can show from Table 2-1 that  $1312/2537 = 51.8\%$  of the strength of the  $00^0_1 \leftarrow 10^0_0$  system lies below  $939 \text{ cm}^{-1}$ , the center of the main band. From theory, we expect approximately 48.8% of the strength of a single  $\Sigma \leftarrow \Sigma$  band of a rigid rotator to occur in the P-branch on the low wavenumber side of the center. The additional strength observed in the P-branch can be attributed to the associated difference bands, primarily the  $01^1_1 \leftarrow 11^1_0$  band which is shifted toward lower wavenumbers by approximately  $20 \text{ cm}^{-1}$  relative to the  $00^0_1 \leftarrow 10^0_0$  band. A similar comparison can not be made reliably for the other band system between 1000 and  $1100 \text{ cm}^{-1}$  because of the interference of the  $02^0_0$  band.

The lines of the  $00^0_1 \leftarrow 10^0_0$  band are the only ones in this region that are strong enough to meet our criterion for consideration in absorption by the earth's atmosphere. Spectral curves showing much of the line structure in the region of this band are shown in Figs. 2-4 and 2-5. The sample represented in Fig. 2-4 was at sufficiently low pressure and long path that the contribution of the weak lines of the associated difference bands provide a significant portion of the absorption and modify the shape of the spectral curve. The absorbance minimum near the band center at  $939 \text{ cm}^{-1}$  is apparent, but an envelope curve connecting the points of maximum absorbance is not smooth as it usually is for a band of this type when the sample pressure is higher. Several unresolved, weak lines of difference bands are intermingled with the main lines and produce the irregular structure. When the pressure is low, the lines are narrow and the maximum amount of absorbance observed with a finite spectral slitwidth depends strongly on the separation between the lines contributing most of the absorption.

Spectral curves in the wings of the band are shown in Fig. 2-5 for a larger sample. The influence of unresolved weak lines is also apparent in these curves, particularly between  $850$  and  $905 \text{ cm}^{-1}$ .

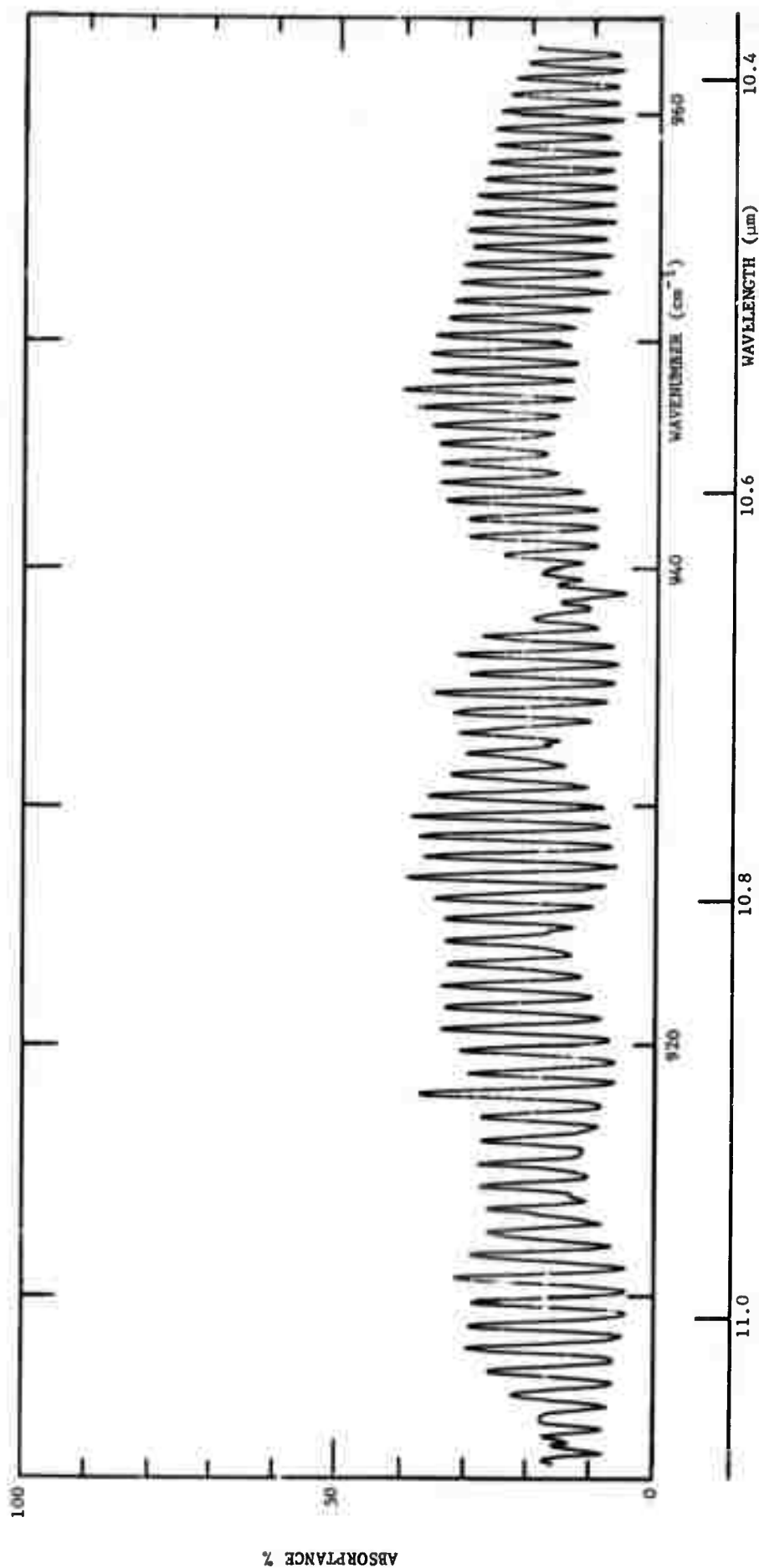


FIG. 2-4. Spectral curve of absorbance from 905 to 960  $\text{cm}^{-1}$ . The sample was 0.0267 atm of pure  $\text{N}_2\text{O}$  at  $296^\circ\text{K}$ .  $L = 477 \text{ m}$ ;  $u = 3.16 \times 10^{22}$  molecules/ $\text{cm}^3$ . Spectral slitwidth is approximately  $0.4 \text{ cm}^{-1}$ .

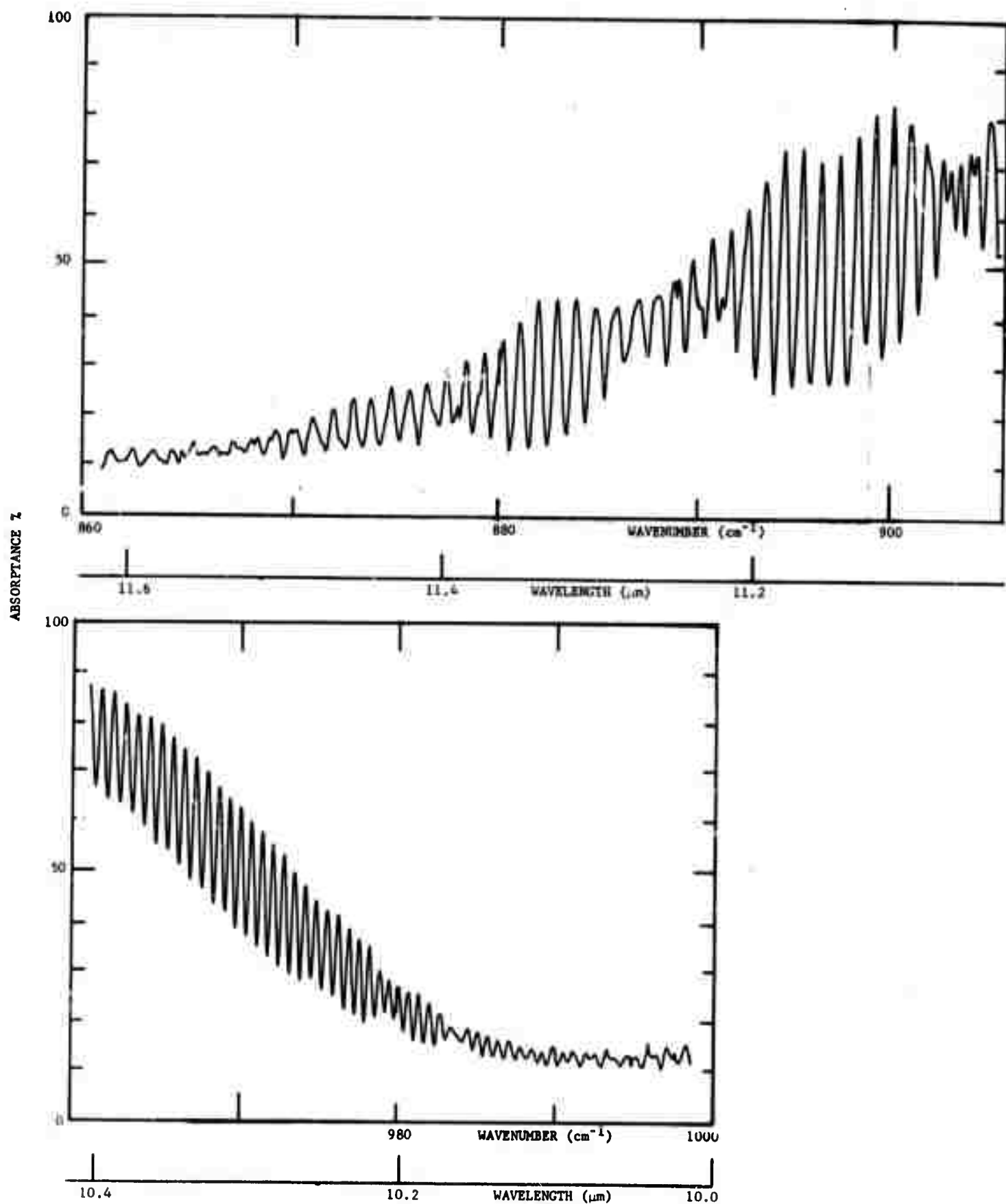


FIG. 2-5. Spectral curve of absorbance from 860 to 905  $\text{cm}^{-1}$  and from 961 to 1000  $\text{cm}^{-1}$ . The sample was 0.20 atm of pure  $\text{N}_2\text{O}$  at 296°K.  $\gamma = 477$  m;  $u = 2.37 \times 10^{23}$  molecules/ $\text{cm}^2$ . Spectral slitwidth is approximately 0.4  $\text{cm}^{-1}$ .

### SECTION 3

#### ABSORPTION BETWEEN 1100 AND 1350 $\text{cm}^{-1}$

Most of the absorption in this region is due to the  $02^00 \leftarrow 00^00$ , and  $10^00 \leftarrow 00^00$  bands centered at 1168.134 and 1284.907  $\text{cm}^{-1}$ , respectively. The associated difference bands,  $03^10 \leftarrow 01^10$  and  $11^10 \leftarrow 01^10$ , are centered at 1160.291 and 1291.501  $\text{cm}^{-1}$ , respectively. Figures 3-1 and 3-2 show spectral curves of transmittance for samples at sufficiently high pressure that the line structure is smoothed out. The corresponding curves of  $(-1/u) \ln T$  appear in Figs. 3-3 and 3-4.

Values of the cumulative integral  $\int_{\nu'}^{\nu} (-1/u) \ln T d\nu$  are listed for several values of  $\nu$  in Table 3-1. From this table, we see that the strength of the  $02^00 \leftarrow 00^00$  band system is  $38.5 \times 10^{-20}$  molecules $^{-1}\text{cm}^2\text{cm}^{-1}$ , the value of the integral from  $\nu' = 1110$  to  $\nu = 1235$   $\text{cm}^{-1}$ . The strength of the system containing the  $10^00 \leftarrow 00^00$  band is  $996 \times 10^{-20}$  molecules $^{-1}\text{cm}^2\text{cm}^{-1}$ . The estimated uncertainty is  $\pm 4\%$  for both of these values which compare favorably with the corresponding values  $40.5 \times 10^{-20}$  and  $986 \times 10^{-20}$  molecules $^{-1}\text{cm}^2\text{cm}^{-1}$  reported by Goody and Wormell<sup>6</sup>.

Figures 3-5 to 3-10 show spectral curves of a variety of samples at sufficiently low pressures that much of the line structure is retained. The influence of the difference bands on the spectral curves is apparent. Part of the feature near 1160  $\text{cm}^{-1}$  is undoubtedly due to the Q-branch of the  $03^10 \leftarrow 01^10$  band associated with the  $02^00 \leftarrow 00^00$  band; i.e., both bands involve the same changes in vibrational quantum numbers. The feature near 1292  $\text{cm}^{-1}$  is due to the Q branch of the  $11^10 \leftarrow 01^10$  difference band. Other lines of the difference bands are also apparent in different portions of the spectrum. The curve shown in Fig. 3-7 was obtained with a narrower slitwidth than were the other curves and consequently contains more structure. Different panels in the same figure represent different spectral

regions. The portion between the vertical broken line and the nearest edge of the panel is repeated in the adjacent panel.

Values of the cumulative integral of absorptance are listed in Tables 3-2 and 3-3 for the samples represented in Figs. 3-5 to 3-10. The sample numbers are given in the figures, and the sample parameters are listed in the figure legends.

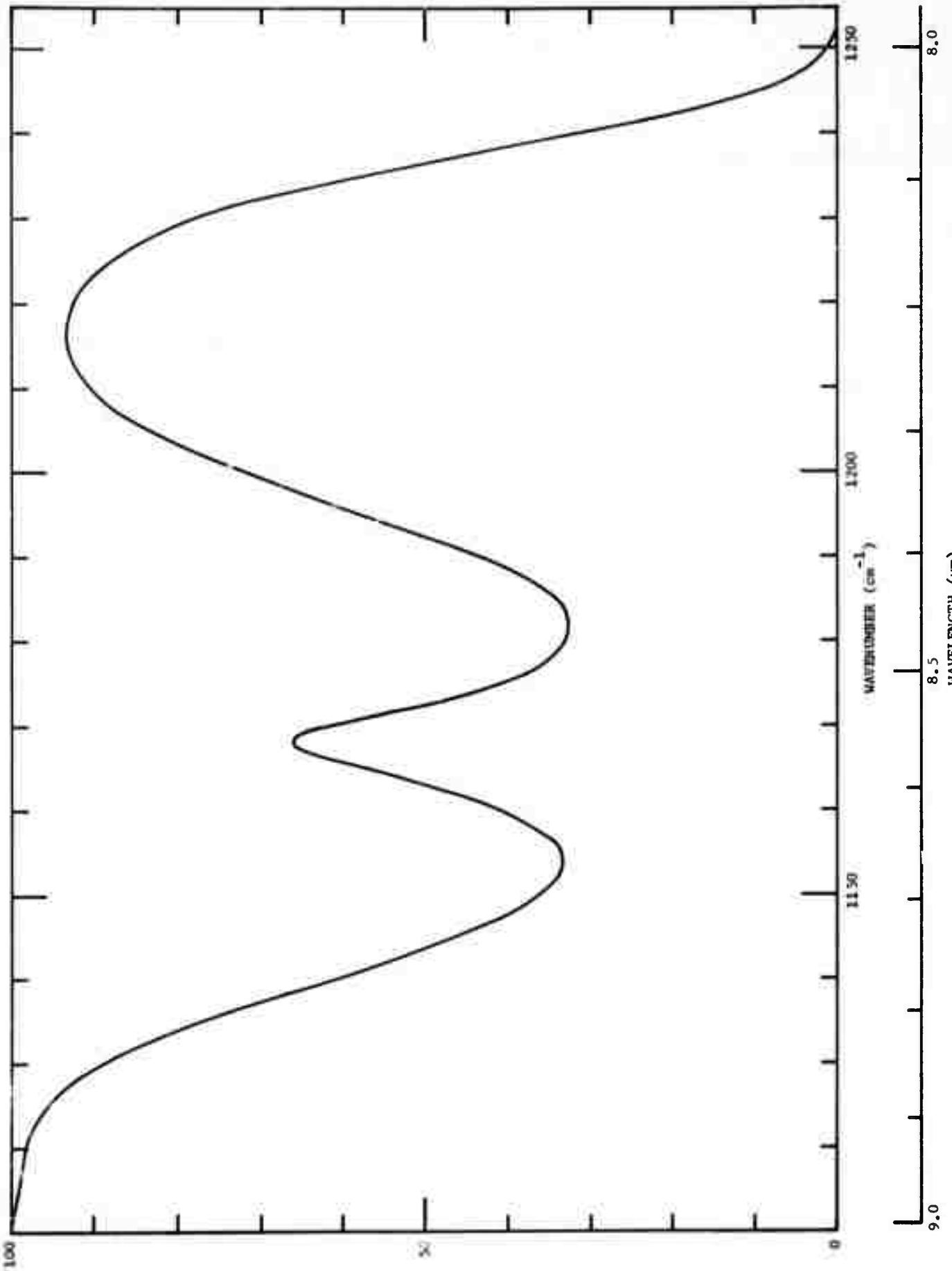


FIG. 3-1. Spectral curve of transmittance from 1110 to 1250  $cm^{-1}$ .  $u = 1.50 \times 10^{20}$  molecules/ $cm^2$ ,  $L = 0.602$  cm, Temp. = 304°K,  $p = 9.84$  atm pure  $N_2O$ . Spectral slitwidth  $\approx 1$   $cm^{-1}$ .

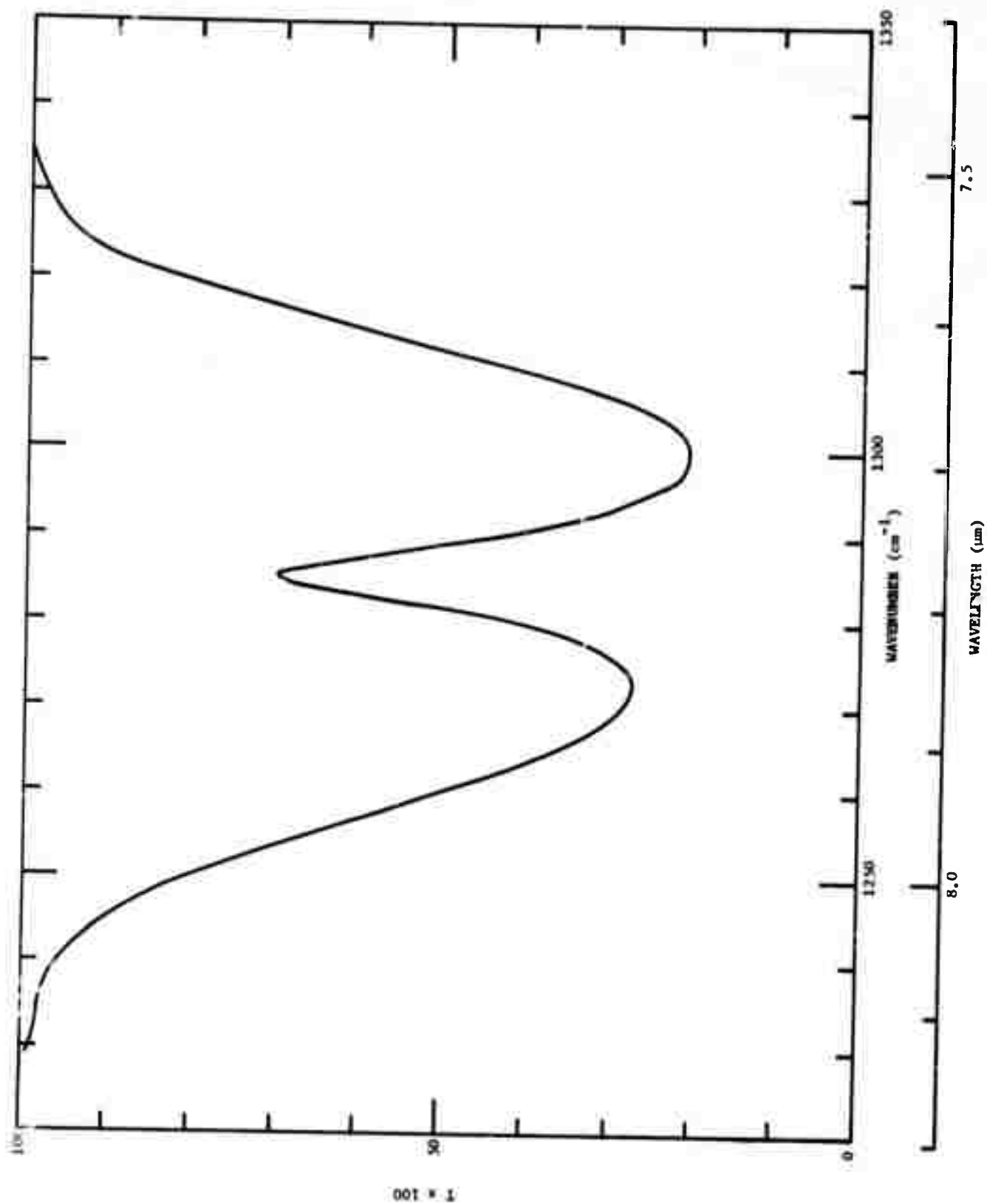


FIG. 3-2. Spectral curve of transmittance from 1220 to 1350  $\text{cm}^{-1}$ .  $u = 0.0647 \times 10^{20}$  molecules/ $\text{cm}^2$ ,  $L = 0.602$  cm, Temp. = 302°K  
 $p = 0.441$  atm with  $\text{N}_2$  added to give a total pressure  $P = 10.59$  atm. Spectral slitwidth  $\sim 0.8$   $\text{cm}^{-1}$ .



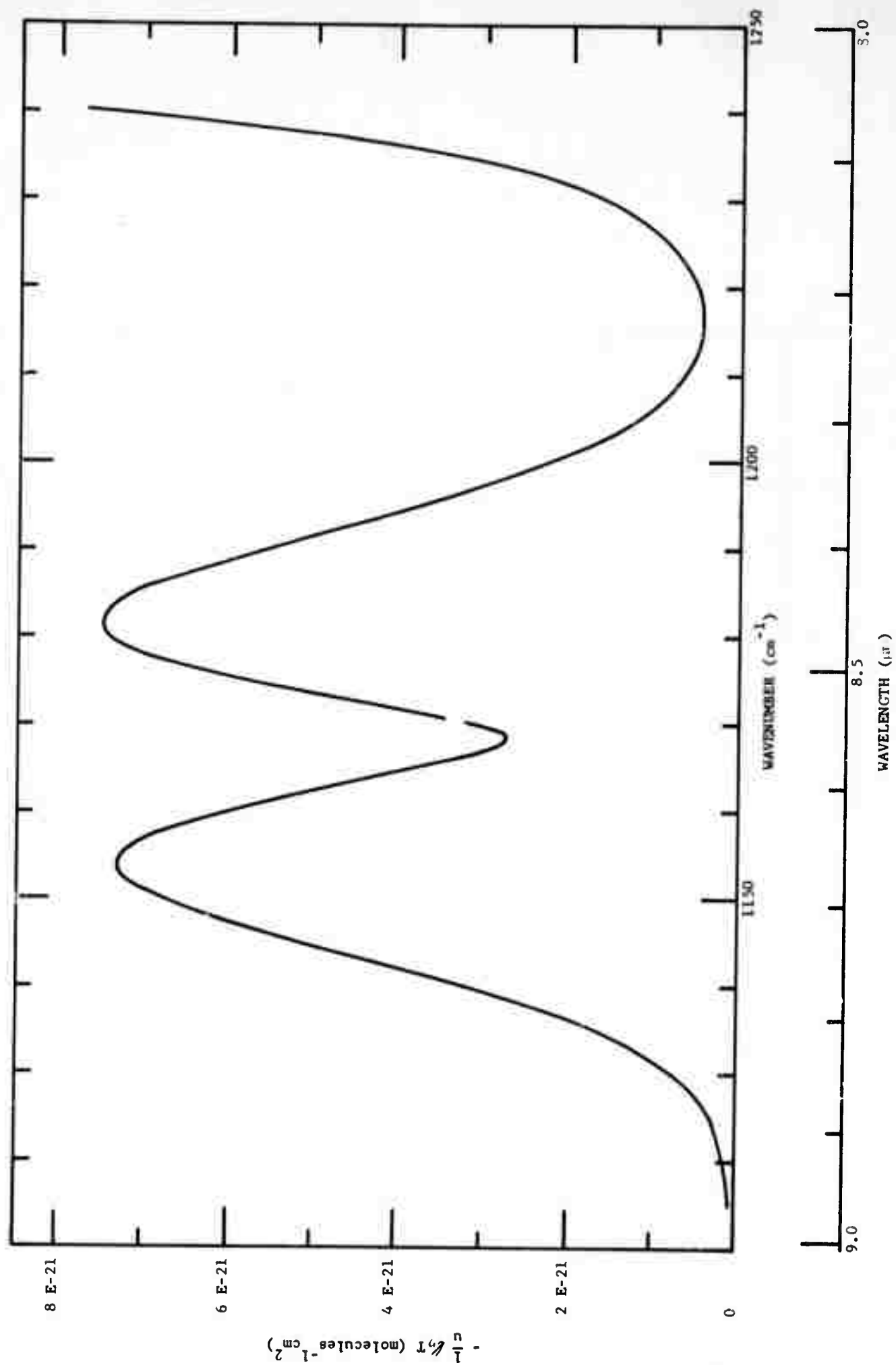


FIG. 3-3. Spectral curve of  $(-1/u) \frac{d^2 T}{du^2}$  for  $\text{N}_2\text{O}$  from 1110 to 1250  $\text{cm}^{-1}$ .

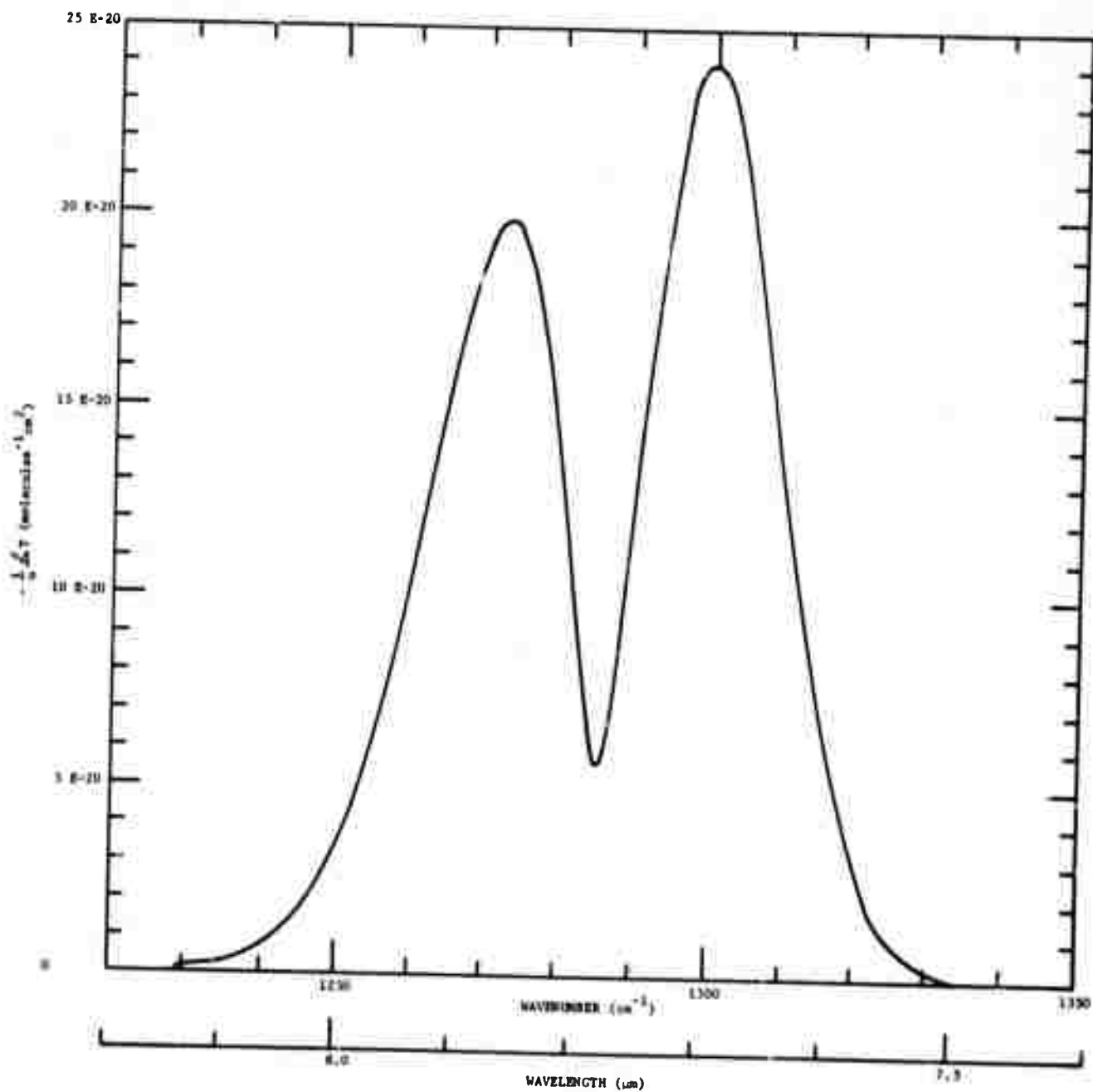


FIG. 3-4. Spectral curve of  $(-1/u) \frac{dT}{d\lambda}$  for  $N_2O$  from 1220 to 1350  $cm^{-1}$ .

TABLE 3-1

INTEGRATED ABSORPTION COEFFICIENT  
BETWEEN 1110 and 1335  $\text{cm}^{-1}$

Multiply all values of the integral by  $10^{-22}$  molecules $^{-1}$   $\text{cm}^2 \text{cm}^{-1}$

$\nu$ ( $\text{cm}^{-1}$ )	$\int_{\nu'}^{\nu} \frac{1}{u} (-\ln T) d\nu$ $\nu' = 1110 (\text{cm}^{-1})$	$\nu$ ( $\text{cm}^{-1}$ )	$\int_{\nu'}^{\nu} \frac{1}{u} (-\ln T) d\nu$ $\nu' = 1230 (\text{cm}^{-1})$
1115	2.464	1240	396.02
1120	7.132	1245	943.17
1125	17.008	1250	2127.17
1130	41.473	1255	4514.95
1135	100.002	1260	8715.40
1140	221.625	1265	15219.14
1145	431.254	1270	23978.49
1150	732.638	1275	33824.89
1155	1090.493	1280	42226.34
1160	1426.870	1285	46726.19
1165	1670.950	1290	50820.09
1170	1823.011	1295	59439.37
1175	2050.138	1300	71060.17
1180	2391.468	1305	82442.49
1185	2761.407	1310	90916.23
1190	3081.160	1315	95872.33
1195	3311.339	1320	98312.92
1200	3457.245	1325	99246.15
1205	3539.731	1330	99539.19
1210	3583.604	1335	99603.51
1215	3610.055		
1220	3633.258		
1225	3665.461		
1230	3724.761		
1235	3845.686		

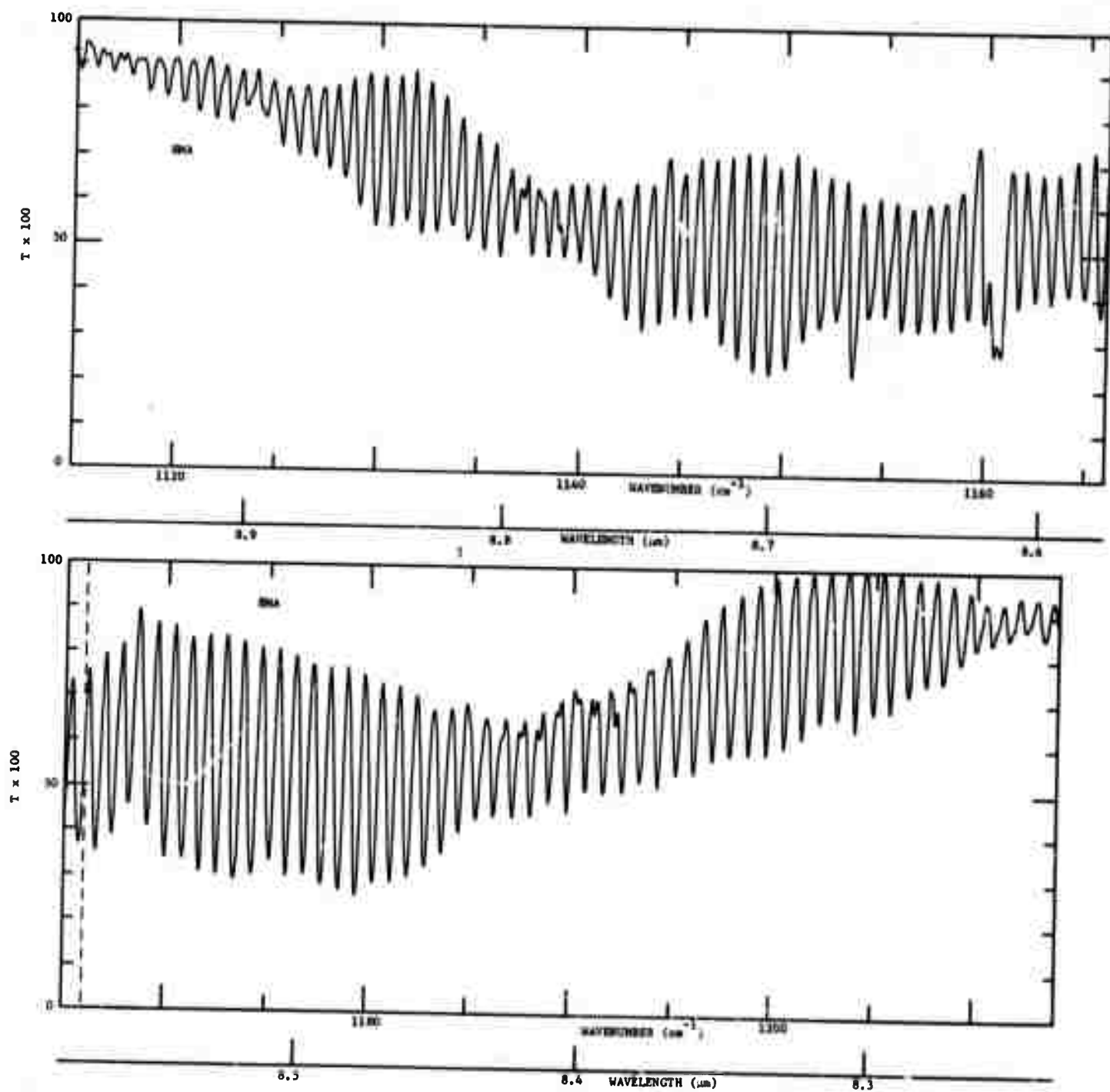


FIG. 3-5. Spectral curve of transmittance from 1115 to  $1300\text{ cm}^{-1}$ .  $u = 31.0 \times 10^{20}$  molecules/ $cm^2$ ,  $L = 123.4\text{ m}$ , Temp. =  $296^\circ K$ ,  $p = 0.0101\text{ atm}$  pure  $N_2O$ . Spectral slitwidth  $\approx 0.3\text{ cm}^{-1}$ .

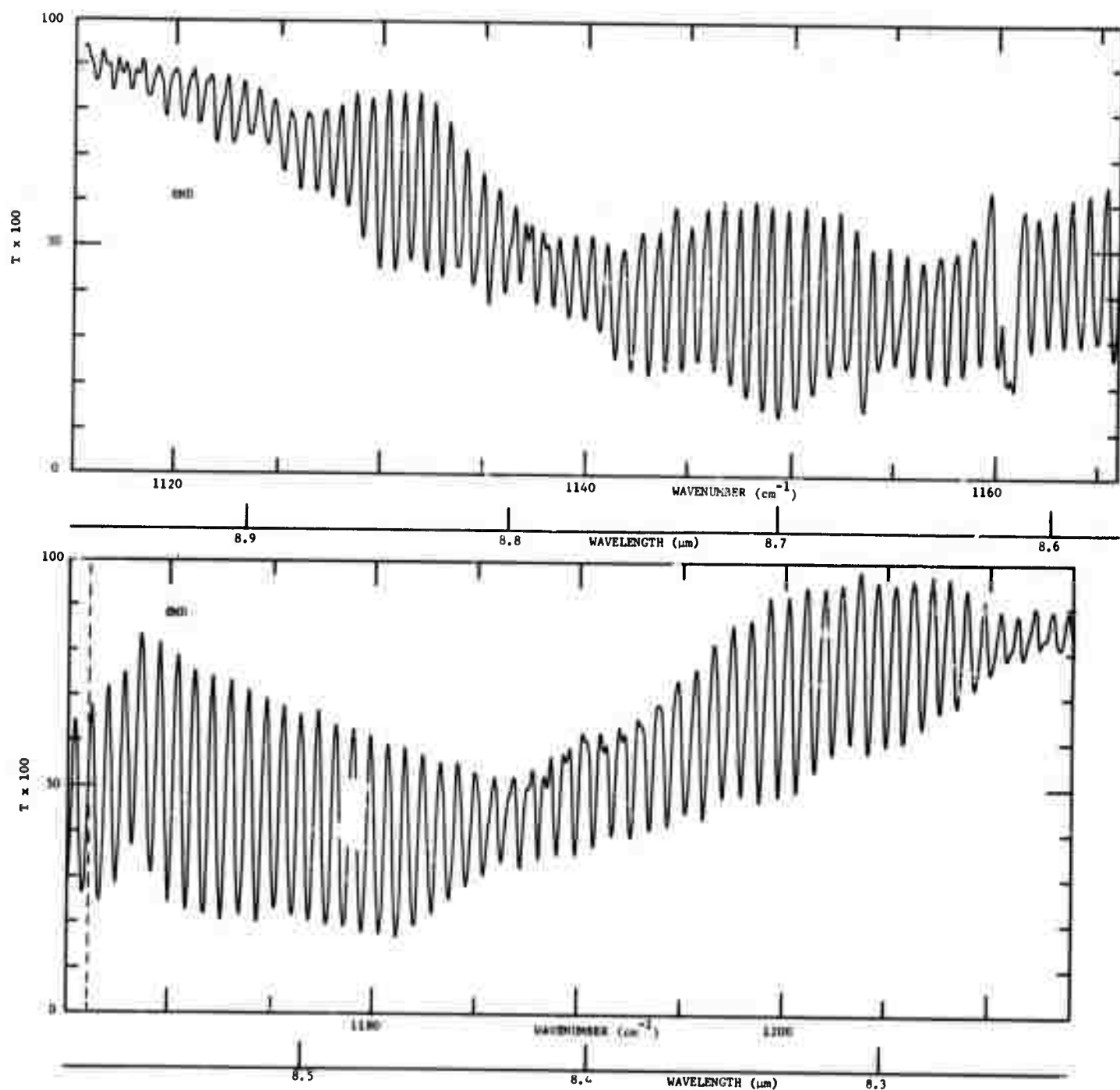


FIG. 3-6. Spectral curve of transmittance from 1115 to 1230  $cm^{-1}$ .  $\rho = 41.5 \times 10^{20}$  molecules/ $cm^2$ ,  $L = 123.4$  m, Temp. = 296°K,  $p = 0.0136$  atm pure  $N_2O$ . Spectral slitwidth = 0.3  $cm^{-1}$ .

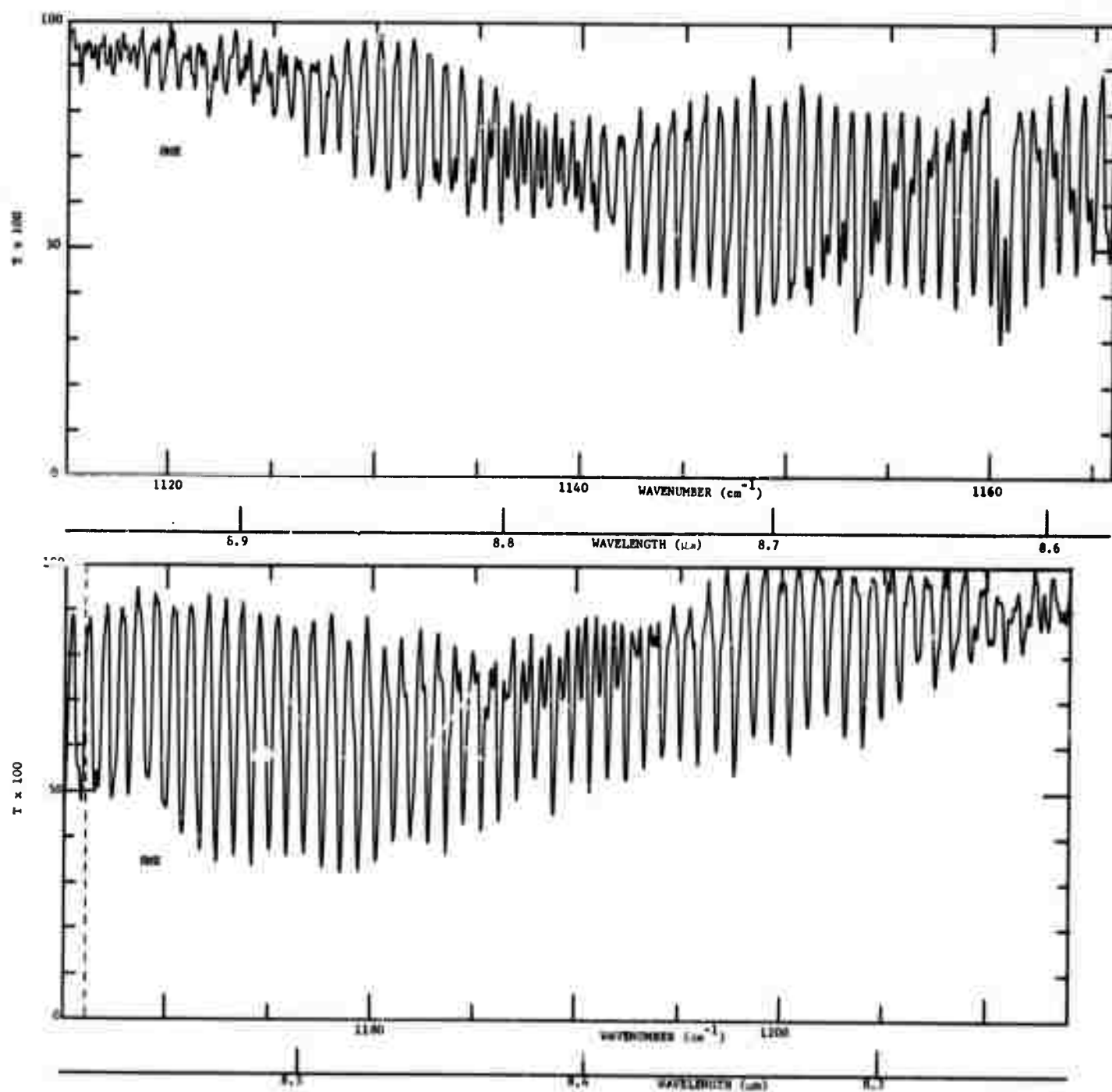


FIG. 3-7. Spectral curve of transmittance from 1115 to 1215  $cm^{-1}$ .  $u = 20.9 \times 10^{20}$  molecules/ $cm^2$ ,  $L = 123.4$  m, Temp = 296°K,  $p = 0.0068$  atm pure  $N_2O$ . Spectral slitwidth  $\approx 0.2$   $cm^{-1}$ .

TABLE 3-2

$$\left[ \int_{\nu}^{\nu} A(\nu) d\nu \right] (\nu = 1115 \text{ cm}^{-1})$$

Sam. No. p (atm) u (#/cm <sup>2</sup> )	8MA 0.0101 31.0 E20	8MD 0.0136 41.5 E20	8ME 0.0068 20.9 E20	Sam. No. p (atm) u (#/cm <sup>2</sup> )	8MA 0.0101 31.0 E20	8MD 0.0136 41.5 E20	8ME 0.0068 20.9 E20
$\nu$ (cm <sup>-1</sup> )				$\nu$ (cm <sup>-1</sup> )			
1115	0	0	0	1165	18,621	23,001	13,540
1116	0,061	0,093	0,057	1166	19,081	23,567	13,879
1117	0,173	0,207	0,130	1167	19,491	24,072	14,163
1118	0,270	0,327	0,203	1168	19,874	24,536	14,435
1119	0,385	0,459	0,276	1169	20,210	24,943	14,650
1120	0,501	0,603	0,357	1170	20,620	25,437	14,967
1121	0,632	0,761	0,441	1171	21,044	25,940	15,314
1122	0,751	0,944	0,553	1172	21,441	26,435	15,605
1123	0,944	1,144	0,654	1173	21,834	26,933	15,901
1124	1,093	1,339	0,743	1174	22,267	27,473	16,242
1125	1,272	1,564	0,874	1175	22,751	28,049	16,614
1126	1,485	1,838	1,009	1176	23,227	28,641	16,978
1127	1,710	2,122	1,146	1177	23,692	29,215	17,301
1128	1,920	2,390	1,303	1178	24,146	29,780	17,635
1129	2,162	2,686	1,464	1179	24,599	30,346	17,955
1130	2,465	3,056	1,669	1180	25,073	30,952	18,343
1131	2,741	3,399	1,845	1181	25,576	31,584	18,735
1132	2,999	3,719	2,036	1182	26,100	32,235	19,130
1133	3,334	4,132	2,264	1183	26,651	32,854	19,490
1134	3,667	4,553	2,524	1184	27,067	33,444	19,815
1135	4,012	4,986	2,765	1185	27,487	34,012	20,127
1136	4,390	5,461	3,040	1186	27,920	34,583	20,456
1137	4,805	5,972	3,354	1187	28,354	35,142	20,761
1138	5,258	6,480	3,649	1188	28,793	35,695	21,067
1139	5,636	7,016	3,966	1189	29,220	36,231	21,363
1140	6,092	7,597	4,294	1190	29,611	36,729	21,658
1141	6,546	8,183	4,624	1191	29,964	37,190	21,894
1142	7,015	8,780	4,952	1192	30,329	37,647	22,145
1143	7,521	9,400	5,302	1193	30,689	38,092	22,369
1144	8,040	10,033	5,654	1194	31,014	38,511	22,607
1145	8,481	10,602	6,035	1195	31,334	38,914	22,829
1146	8,923	11,157	6,347	1196	31,645	39,321	23,067
1147	9,412	11,769	6,699	1197	31,922	39,686	23,251
1148	9,964	12,428	7,134	1198	32,186	40,024	23,435
1149	10,458	13,036	7,510	1199	32,417	40,336	23,592
1150	10,973	13,674	7,875	1200	32,609	40,602	23,724
1151	11,520	14,340	8,265	1201	32,779	40,841	23,858
1152	12,056	15,000	8,716	1202	32,937	41,070	23,964
1153	12,572	15,632	9,112	1203	33,092	41,290	24,109
1154	13,119	16,280	9,513	1204	33,255	41,506	24,276
1155	13,636	16,926	9,900	1205	33,413	41,741	24,433
1156	14,172	17,587	10,283	1206	33,554	41,956	24,553
1157	14,699	18,237	10,653	1207	33,683	42,140	24,644
1158	15,187	18,847	11,008	1208	33,800	42,295	24,749
1159	15,664	19,440	11,342	1209	33,938	42,473	24,851
1160	16,122	20,006	11,687	1210	34,074	42,666	24,970
1161	16,783	20,759	12,216	1211	34,193	42,843	25,101
1162	17,216	21,297	12,531	1212	34,300	43,003	25,214
1163	17,663	21,846	12,846	1213	34,393	43,145	25,266
1164	18,141	22,415	13,177	1214	34,499	43,292	25,373

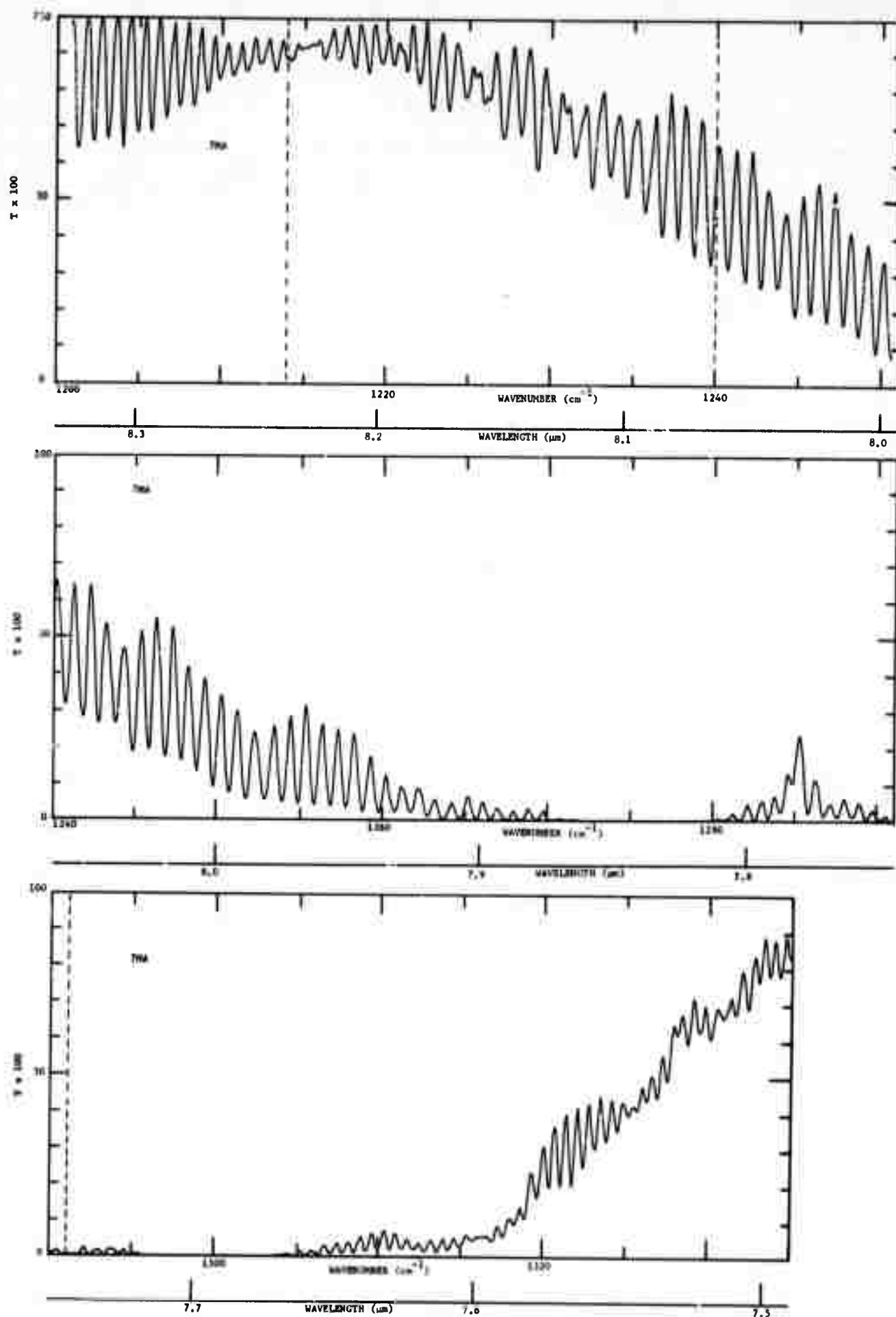


FIG. 3-8. Spectral curves of transmittance from 1200 to 1335  $\text{cm}^{-1}$ .  $u = 31.0 \times 10^{20}$  molecules/ $\text{cm}^2$ ,  $L = 123.4$  m, Temp. = 296°K,  $p = 0.0101$  atm pure  $\text{N}_2\text{O}$ . Spectral slitwidth  $\approx 0.4$   $\text{cm}^{-1}$ .



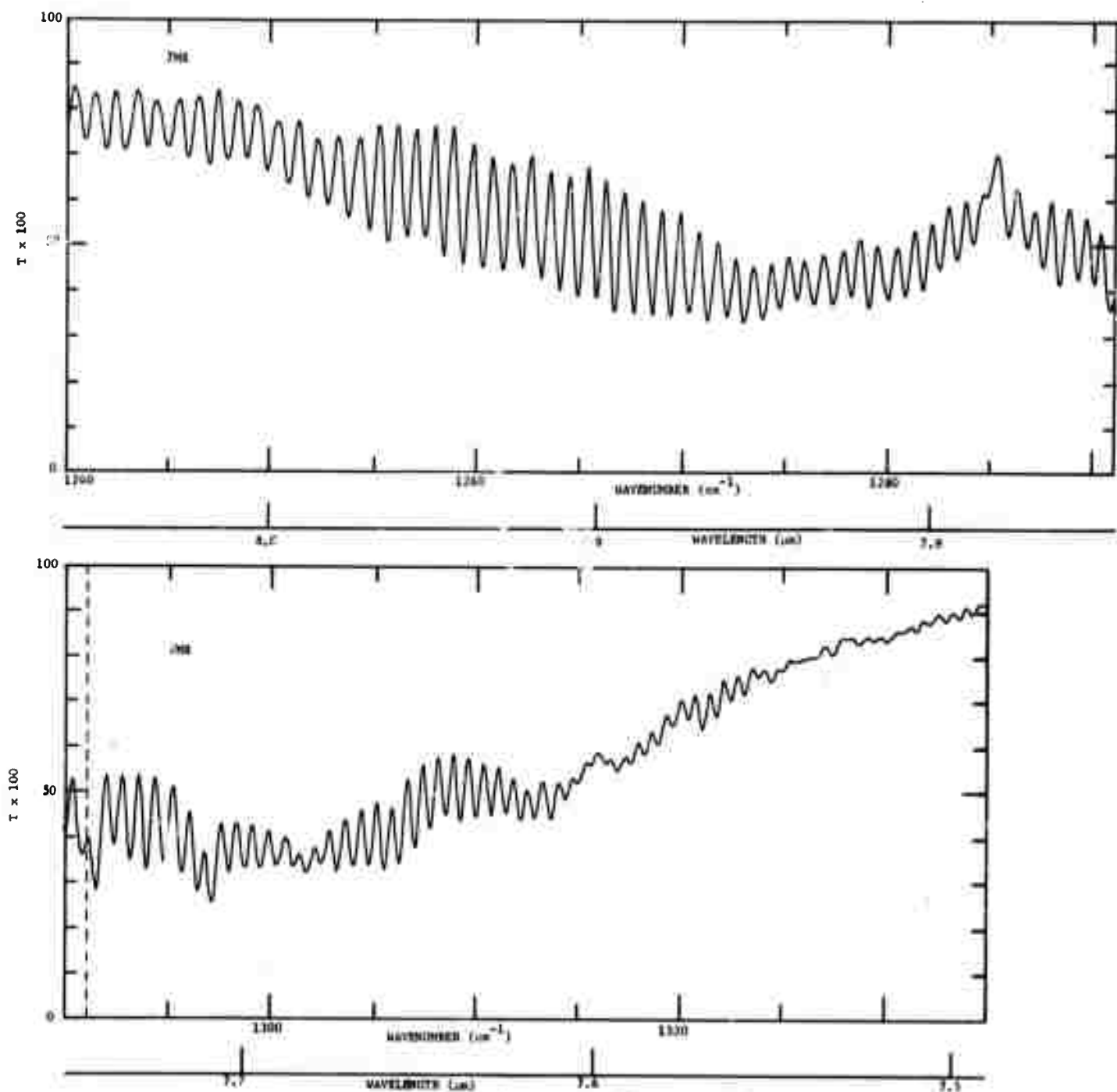


FIG. 3-9. Spectral curve of transmittance from 1240 to 1335  $cm^{-1}$ .  $n = 14.9 \times 10^{19}$  molecules/ $cm^2$ ,  $l = 0.77$  m, Temp. = 296°K,  $p = 0.00126$  atm pure  $N_2O$ . Spectral slitwidth  $\approx 0.45$   $cm^{-1}$ .

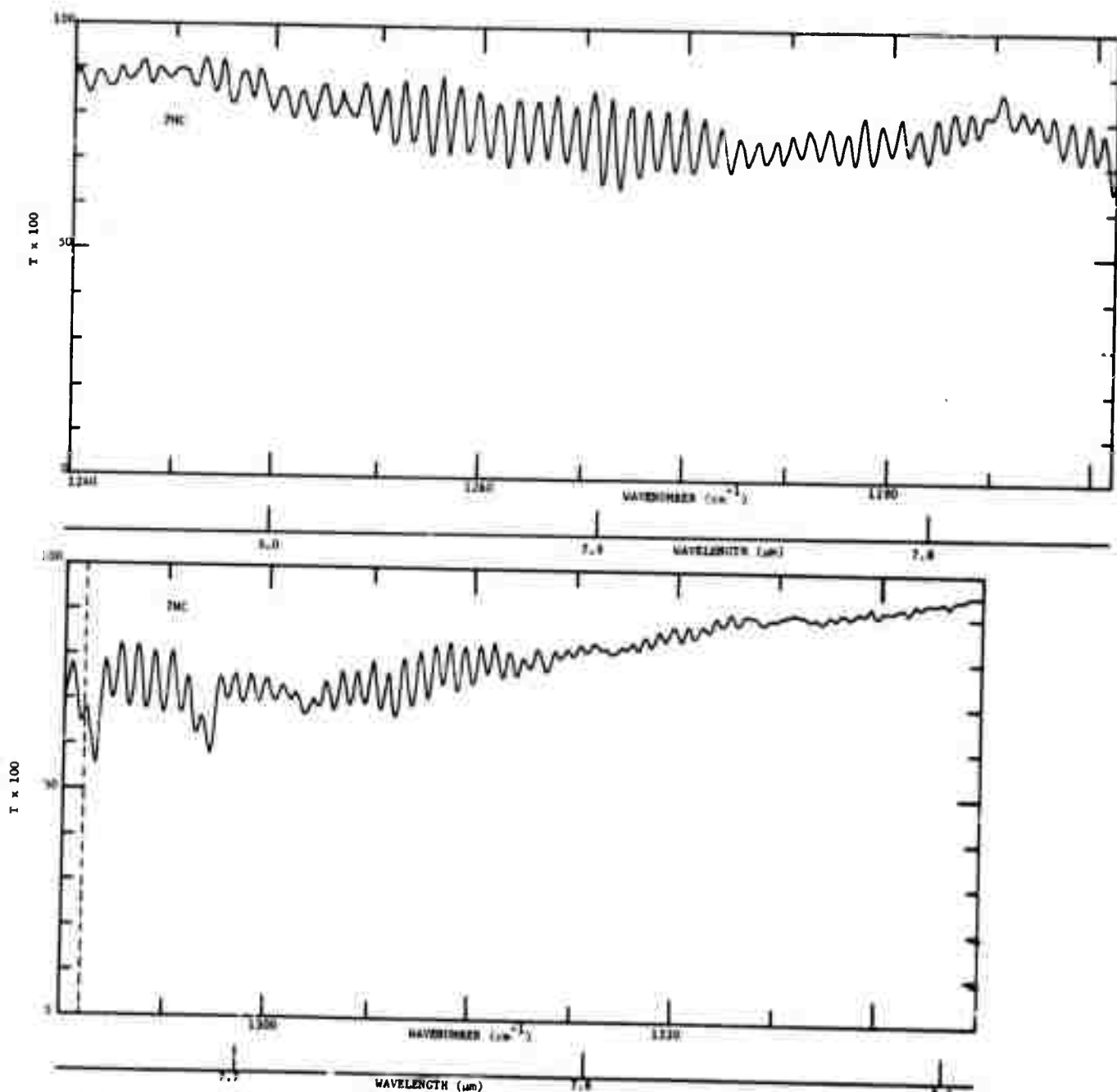


FIG. 3-10. Spectral curve of transmittance from 1240 to 1335  $cm^{-1}$ .  $u = 4.98 \times 10^{20}$  molecules/ $cm^2$ ,  $L = 477$  m, Temp. = 296°K,  $p = 0.00042$  atm pure  $N_2O$ . Spectral slitwidth  $\approx 0.45$   $cm^{-1}$ .

TABLE 3-3

$$[\int_{v'}^v A(v)dv] \quad (v'=1240 \text{ cm}^{-1})$$

Sam. No. p (atm) u (#/cm <sup>2</sup> )	7MA 0.0101 31.0 E20	7MB 0.00126 14.9 E20	7MC 0.00042 4.98 E20	Sam. No. p (atm) u (#/cm <sup>2</sup> )	7MA 0.0101 31.0 E20	7MB 0.00126 14.9 E20	7MC 0.00042 4.98 E20
v (cm <sup>-1</sup> )				v (cm <sup>-1</sup> )			
1240	0	0	0	1295	48,961	24,316	11,746
1241	0,519	0,209	0,134	1296	49,957	24,593	12,009
1242	1,068	0,433	0,263	1297	50,954	25,252	12,349
1243	1,624	0,663	0,381	1298	51,954	25,905	12,666
1244	2,228	0,885	0,491	1299	52,954	26,525	12,941
1245	2,825	1,119	0,604	1300	53,954	27,142	13,209
1246	3,527	1,355	0,723	1301	54,954	27,770	13,467
1247	4,170	1,596	0,839	1302	55,954	28,426	13,709
1248	4,829	1,838	0,973	1303	56,954	29,050	14,078
1249	5,553	2,080	1,104	1304	57,952	29,672	14,359
1250	6,339	2,339	1,258	1305	58,946	30,276	14,627
1251	7,101	2,629	1,429	1306	59,934	30,860	14,890
1252	7,932	2,937	1,608	1307	60,916	31,435	15,163
1253	8,782	3,271	1,777	1308	61,894	31,958	15,411
1254	9,624	3,620	1,959	1309	62,860	32,430	15,614
1255	10,473	3,971	2,142	1310	63,824	32,931	15,840
1256	11,305	4,317	2,338	1311	64,776	33,427	16,049
1257	12,162	4,668	2,528	1312	65,739	33,924	16,254
1258	13,030	5,025	2,732	1313	66,710	34,456	16,469
1259	13,905	5,404	2,933	1314	67,674	34,968	16,670
1260	14,815	5,806	3,149	1315	68,639	35,456	16,857
1261	15,750	6,239	3,381	1316	69,594	35,892	17,031
1262	16,693	6,677	3,613	1317	70,529	36,326	17,210
1263	17,643	7,117	3,843	1318	71,445	36,746	17,382
1264	18,615	7,592	4,073	1319	72,327	37,136	17,544
1265	19,580	8,076	4,320	1320	73,191	37,470	17,685
1266	20,555	8,550	4,562	1321	73,837	37,785	17,826
1267	21,531	9,045	4,819	1322	74,524	38,091	17,952
1268	22,515	9,554	5,065	1323	75,189	38,358	18,064
1269	23,502	10,078	5,311	1324	75,815	38,599	18,167
1270	24,488	10,613	5,558	1325	76,419	38,835	18,278
1271	25,482	11,174	5,819	1326	76,990	39,045	18,375
1272	26,479	11,753	6,069	1327	77,518	39,240	18,478
1273	27,479	12,356	6,306	1328	77,946	39,415	18,581
1274	28,479	12,969	6,641	1329	78,298	39,575	18,676
1275	29,479	13,559	6,908	1330	78,650	39,734	18,765
1276	30,479	14,124	7,160	1331	78,984	39,880	18,850
1277	31,479	14,699	7,410	1332	79,263	40,010	18,928
1278	32,479	15,272	7,669	1333	79,504	40,123	18,995
1279	33,479	15,831	7,918	1334	79,670	40,224	19,058
1280	34,479	16,402	8,170	1335	79,839	40,312	19,109
1281	35,473	16,960	8,407	1336	79,979	40,389	19,157
1282	36,458	17,489	8,657	1337	80,112	40,468	19,201
1283	37,429	17,974	8,876	1338	80,193	40,522	19,240
1284	38,389	18,437	9,084	1339	80,227	40,582	19,281
1285	39,297	18,858	9,265	1340	80,364	40,639	19,320
1286	40,164	19,237	9,457	1341	80,432	40,687	19,351
1287	41,103	19,677	9,653	1342	80,451	40,721	19,368
1288	42,068	20,145	9,859	1343	80,462	40,753	19,380
1289	43,032	20,638	10,095	1344	80,466	40,778	19,368
1290	44,010	21,153	10,348	1345	80,466	40,797	19,388
1291	45,021	21,714	10,628				
1292	45,996	22,331	10,976				
1293	46,963	22,867	11,217				
1294	47,971	23,443	11,478				

 Reproduced from  
best available copy.

## SECTION 4

### ABSORPTION BETWEEN 2100 AND 2380 $\text{cm}^{-1}$

Figure 4-1 shows spectral curves of transmittance between 2100 and 2380  $\text{cm}^{-1}$  for a variety of high-pressure samples with the line structure smoothed out. The sample parameters are listed in Table 4-1. The center of the main band,  $00^01 \leftarrow 00^00$ , at 2223.756  $\text{cm}^{-1}$  is apparent, and the transmittance maximum near 2322  $\text{cm}^{-1}$  is probably due to the center of the  $04^00 \leftarrow 00^00$  band. All of the obvious features of other bands are smoothed out because of the high sample pressures.

A spectral plot of the absorption coefficient is shown in Fig. 4-2. This plot does not extend below 2140  $\text{cm}^{-1}$  nor above 2270  $\text{cm}^{-1}$  although absorption was observed in these regions. A large portion of the absorption beyond these limits is due to the extreme wings of the very strong lines centered between 2150 and 2250  $\text{cm}^{-1}$ . As discussed in Section 2, the continuum absorption coefficient for wing absorption increases linearly with pressure. Thus, the values of  $(-1/u) \ln T$  observed beyond these limits increase with increasing pressure and do not represent the intrinsic absorption due to local lines. By investigating several samples covering a wide range of pressures, we were able to account for the wing absorption and to determine the combined strength of the 2223.756  $\text{cm}^{-1}$  band and its associated difference band. Our value is  $5.71 (\pm 0.25) \times 10^{-17} \text{ molecules}^{-1} \text{ cm}^2 \text{ cm}^{-1}$ .

Transmittance curves are shown in Figs. 4-3 and 4-4 for three samples at relatively low pressures so that the line structure is retained. The influence of the difference bands on the curves is apparent. The curves in Fig. 4-5 correspond to a sample at very low pressures so that the contributions by the weak lines are much greater relative to that by the strong lines than is the case at higher pressures. Note that the smooth contour such as that observed in Fig. 4-1 is completely modified, even for the curve obtained with wide slits. The transmittance maximum near the center of the

main band,  $00^0_1 \leftarrow 00^0_0$  is nearly obliterated, and the Q-branch of the  $01^1_1 \leftarrow 01^1_0$  band near 2209 is very prominent. There is also evidence of the Q-branch of the  $02^0_1 \leftarrow 02^0_0$  and  $02^2_1 \leftarrow 02^2_0$  bands, both of which are centered near 2195  $\text{cm}^{-1}$ .

Values of the integrated absorptance are shown in Table 4-3 for the three samples whose transmittance curves are shown in Figs. 4-3 and 4-4. The sample parameters are listed in Table 4-1. Table 4-2 gives  $(-1/u) \int \frac{d\epsilon}{\nu} T d\nu$  for the spectral region from 2145 to 2280.

The absorption at 2290  $\text{cm}^{-1}$  for samples at high pressure is primarily due to the wings of the strong lines of the  $00^0_1 \leftarrow 00^0_0$  band centered between 2230 to 2260  $\text{cm}^{-1}$ . From the transmittance curves shown in Fig. 4-1 for Samples 4M41 and 4M40, we determined the continuum absorption coefficient at 2290  $\text{cm}^{-1}$  due to the wings of the lines:

$$C_s^0 = 7.55 \times 10^{-23} \text{ molecules}^{-1} \text{ cm}^2 \text{ atm}^{-1}.$$

Using the Lorentz line shape, we calculated the absorption coefficient due to the wings of all of the lines of the  $\nu_3$  band. The calculated value,

$$C_s^0 (\text{calc}) = 39.5 \times 10^{-23} \text{ molecules}^{-1} \text{ cm}^2 \text{ atm}^{-1},$$

is much larger than the observed value, indicating that the wings of the lines absorb less than the Lorentz line shape predicts.

We also calculated the continuum absorption coefficient by assuming that the shape of the wings of the lines was the same as that determined previously<sup>7</sup> in our laboratory for self-broadened lines of the  $\nu_3$  band of  $\text{CO}_2$ . This value,

$$C_s^0 = 5.54 \times 10^{-23} \text{ molecules}^{-1} \text{ cm}^2 \text{ atm}^{-1},$$

agrees much better with experiment than does the calculated value based on the Lorentz shape.

Experimental values of the continuum absorption coefficient at 990  $\text{cm}^{-1}$  and 1215  $\text{cm}^{-1}$  were also considerably smaller than the calculated values based on the Lorentz shape. The continuum at these two points is due primarily to the wings of the  $00^0_1 \leftarrow 10^0_0$  and  $10^0_0 \leftarrow 00^0_0$  bands, respectively. We conclude that the wings of self-broadened  $\text{N}_2\text{O}$  lines are quite sub-Lorentzian and may be similar in shape to self-broadened  $\text{CO}_2$  lines.

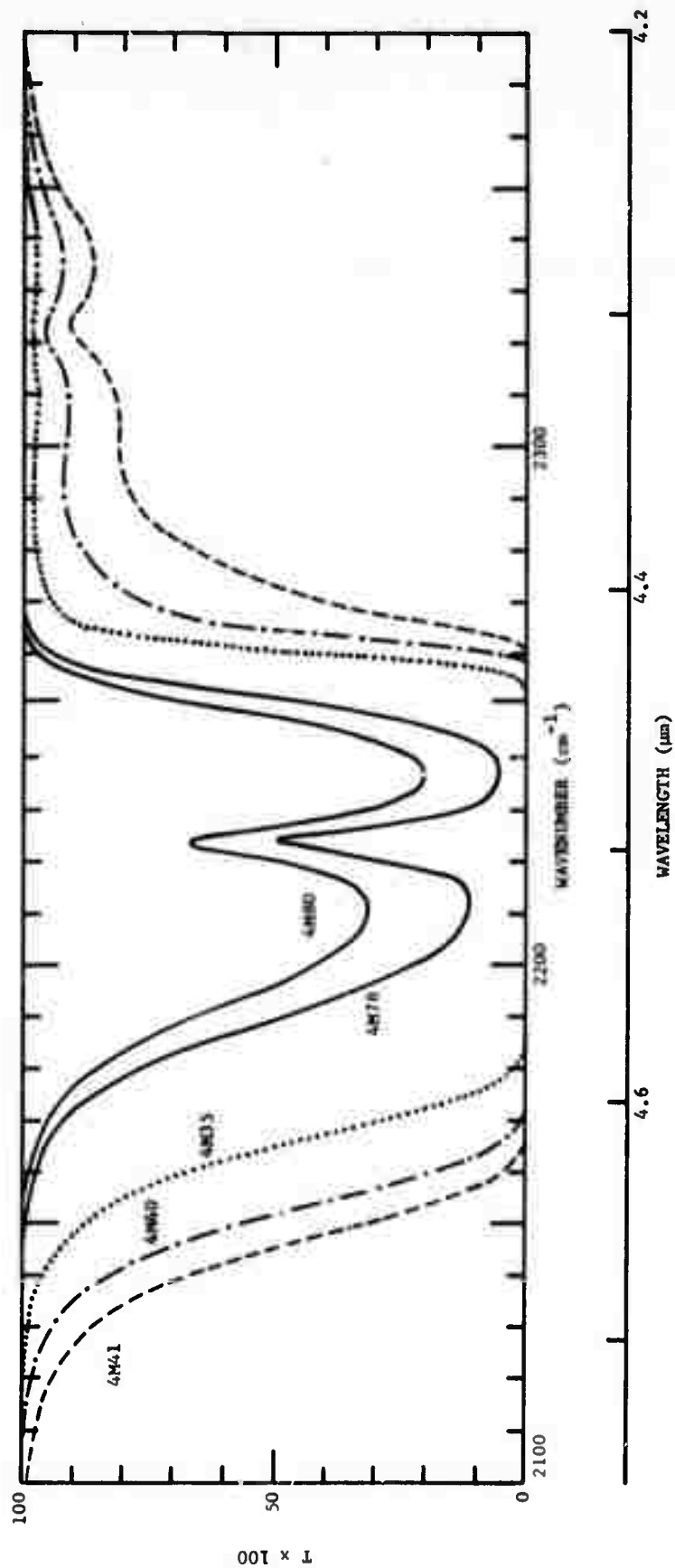


FIG. 4-1. Spectral curve of transmittance from 2100  $\text{cm}^{-1}$  to 2380  $\text{cm}^{-1}$  for several samples at pressures greater than 7 atm. The parameters for each sample are given in Table 4-1. Spectral slitwidth  $\approx 0.3 \text{ cm}^{-1}$ .

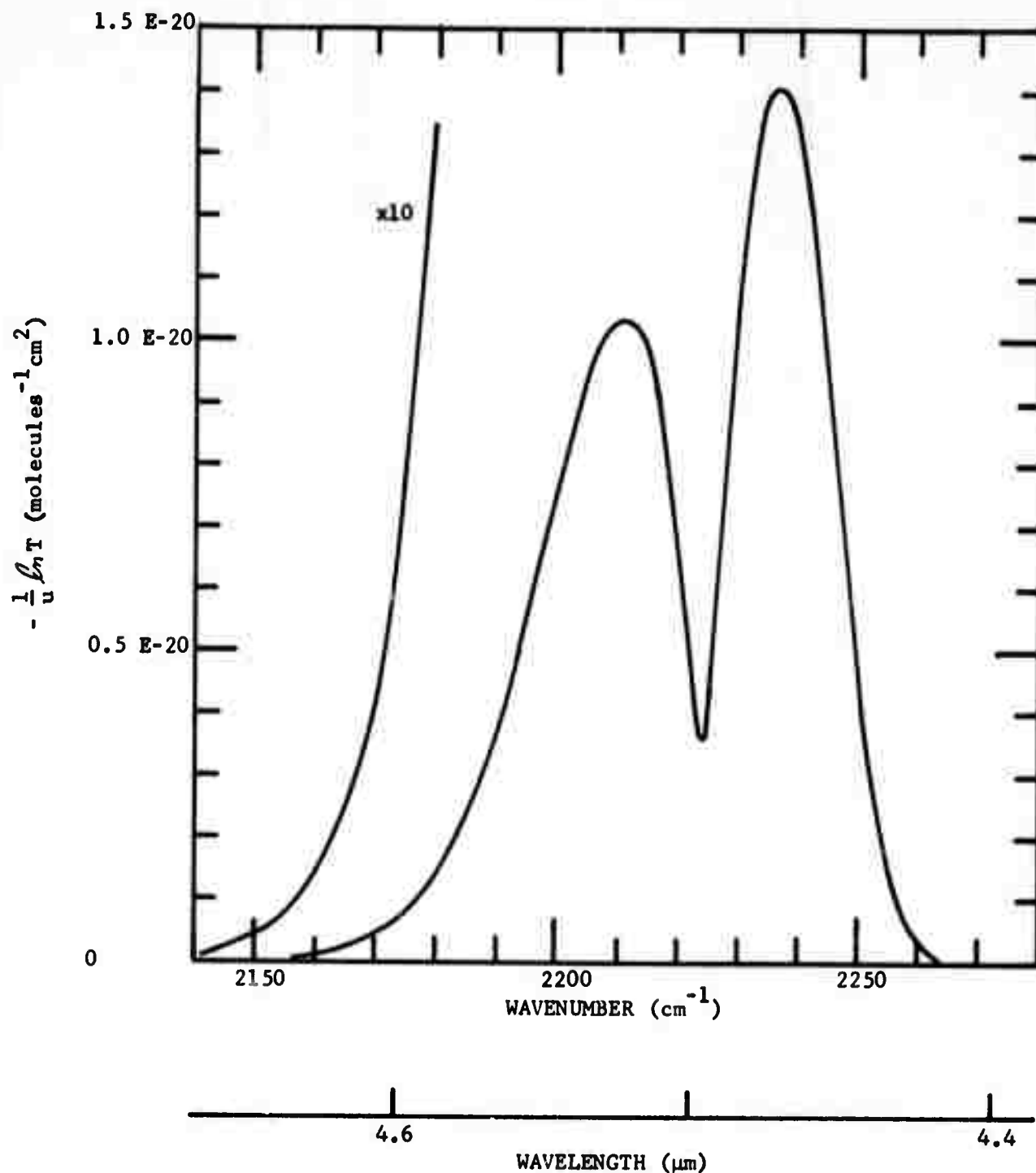


FIG. 4-2. Spectral curves of  $(-1/u) \ln T$  between 2140 and 2280 cm $^{-1}$ . The curves are based on transmittance curves such as those in Fig. 4-1 which represent samples at sufficiently high pressure that the line structure is smoothed out. Values were multiplied by 10 before plotting the points for the left-hand curve.

TABLE 4-1

## SAMPLE PARAMETERS

Sample Number	P atm	P <sub>N<sub>2</sub></sub> atm	P atm	u molecules/cm <sup>2</sup>	Temperature °K	L Meters
4M35	13.59	11.55	2.04	30.1	302	0.00602
4M40	7.80	0	7.80	118.6	302	0.00602
4M41	13.59	0	13.59	212.3	302	0.00602
4M48	0.1250	0	0.1250	1.845	300	0.00602
4M49	0.0625	0	0.0625	0.922	300	0.00602
4M57	0.257	0	0.257	3.77	301	0.00602
4M78	8.03	7.23	0.803	2.00	301	0.00102
4M80	9.03	8.57	0.453	1.12	302	0.00102
4MD	0.000087	0	0.000087	128.0	296	595



TABLE 4-2  
INTEGRATED ABSORPTION COEFFICIENT  
BETWEEN 2145 and 2280  $\text{cm}^{-1}$

---

Multiply all values of the integral by  $10^{-20}$  molecules $^{-1}$   $\text{cm}^2 \text{cm}^{-1}$

---

$\nu$ ( $\text{cm}^{-1}$ )	$\int_{\nu'=2140 \text{ cm}^{-1}}^{\nu} \frac{1}{u} (-\log T) d\nu$
2145	0.534
2150	2.161
2155	4.976
2160	10.513
2165	19.137
2170	34.601
2175	61.879
2180	112.003
2185	199.500
2190	345.034
2195	566.959
2200	886.547
2205	1311.890
2210	1808.910
2215	2321.279
2220	2740.897
2225	2965.134
2230	3324.176
2235	3940.207
2240	4634.130
2245	5188.588
2250	5526.007
2255	5662.765
2260	5700.722
2265	5707.949
2270	5709.411
2275	5710.132
2280	5710.187

TABLE 4-3

$$\left[ \int_{\nu'}^{\nu} A(\nu) d\nu \right] (\nu' = 2162 \text{ cm}^{-1})$$

Sam. No.	4M57	4M48	4M49	Sam. No.	4M57	4M48	4M49
p (atm) <sub>2</sub>	0.257	0.125	0.0625	p (atm) <sub>2</sub>	0.257	0.125	0.0625
u (#/cm <sup>2</sup> )	3.77 E18	1.845 E18	0.922 E18	u (#/cm <sup>2</sup> )	3.77 E 18	1.845 E18	0.922 E18
$\nu$ (cm <sup>-1</sup> )				$\nu$ (cm <sup>-1</sup> )			
2162	0,	0,	0,	2212	16,933	10,215	5,493
2163	0,067	0,027	0,017	2213	19,621	13,602	5,698
2164	0,136	0,057	0,037	2214	20,311	10,987	5,699
2165	0,200	0,085	0,054	2215	21,997	11,364	6,113
2166	0,279	0,124	0,074	2216	21,652	11,781	6,325
2167	0,362	0,171	0,100	2217	22,290	12,146	6,536
2168	0,498	0,228	0,131	2218	22,950	12,520	6,743
2169	0,629	0,291	0,167	2219	23,619	12,896	6,938
2170	0,760	0,357	0,202	2220	24,262	13,266	7,132
2171	0,952	0,414	0,235	2221	24,955	13,579	7,300
2172	1,050	0,484	0,277	2222	25,364	13,663	7,452
2173	1,221	0,566	0,324	2223	25,877	14,151	7,627
2174	1,465	0,648	0,370	2224	26,244	14,332	7,726
2175	1,639	0,743	0,423	2225	26,734	14,597	7,868
2176	1,819	0,845	0,476	2226	27,232	14,869	8,019
2177	2,047	0,957	0,530	2227	27,774	15,175	8,156
2178	2,252	1,063	0,581	2228	28,435	15,566	8,405
2179	2,481	1,163	0,649	2229	29,140	15,963	8,614
2180	2,720	1,316	0,721	2230	29,797	16,334	8,806
2181	3,002	1,463	0,802	2231	30,467	16,739	9,031
2182	3,334	1,642	0,900	2232	31,240	17,188	9,270
2183	3,675	1,817	0,997	2233	31,978	17,604	9,462
2184	4,034	1,998	1,097	2234	32,695	18,037	9,724
2185	4,394	2,188	1,195	2235	33,454	18,479	9,962
2186	4,768	2,381	1,296	2236	34,199	18,894	10,175
2187	5,162	2,587	1,406	2237	34,939	19,332	10,416
2188	5,584	2,813	1,524	2238	35,663	19,749	10,633
2189	6,017	3,041	1,642	2239	36,406	20,146	10,849
2190	6,470	3,297	1,779	2240	37,139	20,574	11,056
2191	6,917	3,551	1,916	2241	37,830	20,944	11,249
2192	7,306	3,763	2,037	2242	38,548	21,351	11,468
2193	7,737	3,999	2,177	2243	39,201	21,688	11,631
2194	8,216	4,271	2,328	2244	39,861	22,064	11,832
2195	8,734	4,559	2,482	2245	40,494	22,378	11,967
2196	9,296	4,873	2,648	2246	41,131	22,700	12,154
2197	9,876	5,178	2,814	2247	41,667	23,010	12,314
2198	10,463	5,504	2,990	2248	42,205	23,267	12,442
2199	11,068	5,840	3,171	2249	42,723	23,539	12,565
2200	11,649	6,180	3,358	2250	43,267	23,786	12,709
2201	12,192	6,492	3,538	2251	43,623	23,991	12,812
2202	12,723	6,772	3,688	2252	44,017	24,162	12,908
2203	13,260	7,102	3,864	2253	44,361	24,360	12,997
2204	13,905	7,455	4,059	2254	44,706	24,521	13,080
2205	14,547	7,815	4,242	2255	44,968	24,552	13,148
2206	15,197	8,169	4,430	2256	45,225	24,764	13,206
2207	15,853	8,534	4,620	2257	45,423	24,657	13,256
2208	16,479	8,888	4,799	2258	45,578	24,930	13,284
2209	17,082	9,209	4,979	2259	45,693	24,986	13,326
2210	17,701	9,552	5,152	2260	45,799	25,030	13,350
2211	18,333	9,670	5,313	2261	45,833	25,059	13,365

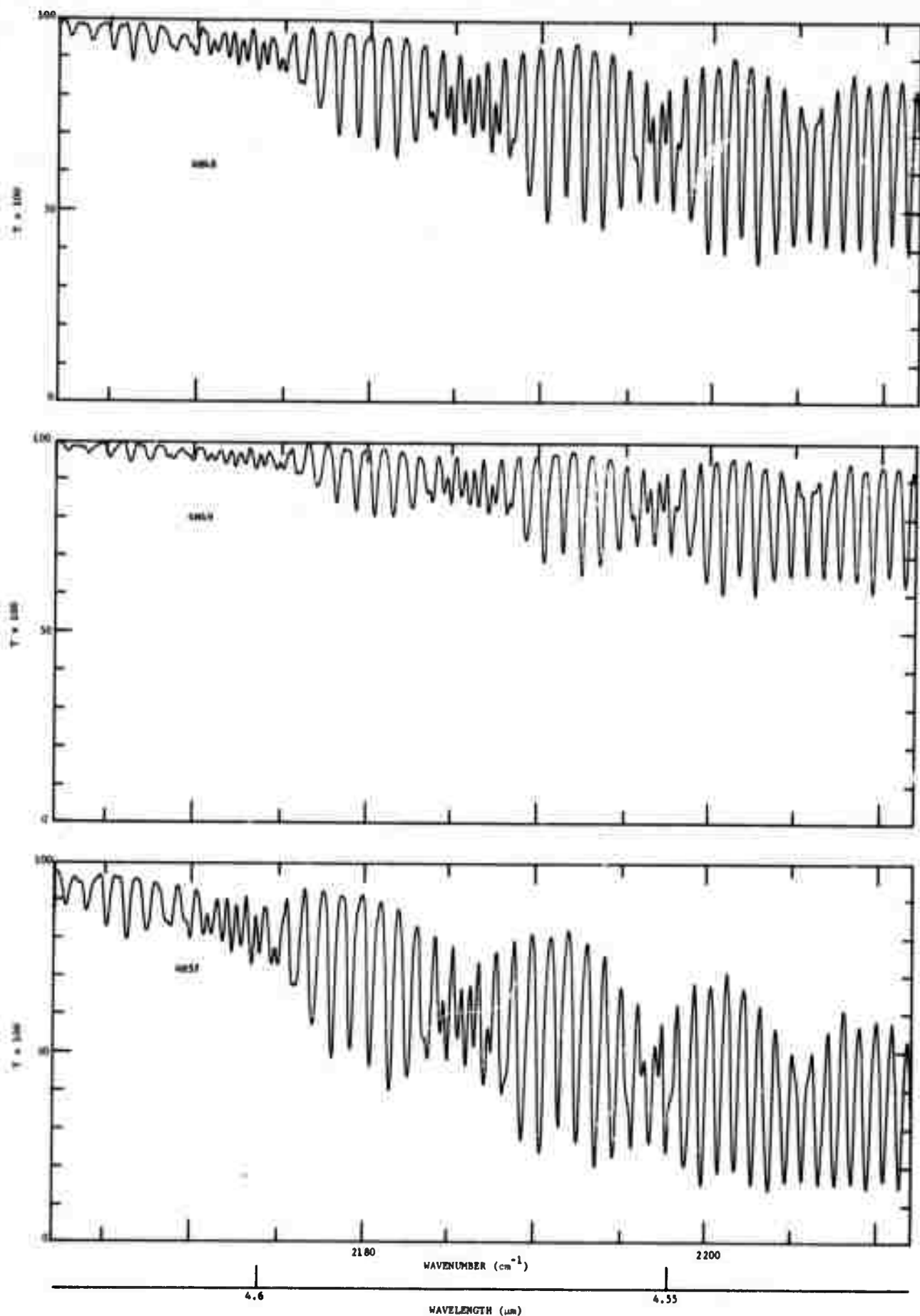


FIG. 4-3. Spectral curves of transmittance between 2165 and 2210  $\text{cm}^{-1}$ . The sample parameters are given in Table 4-1. Spectral slitwidth  $\approx 0.3 \text{ cm}^{-1}$ .

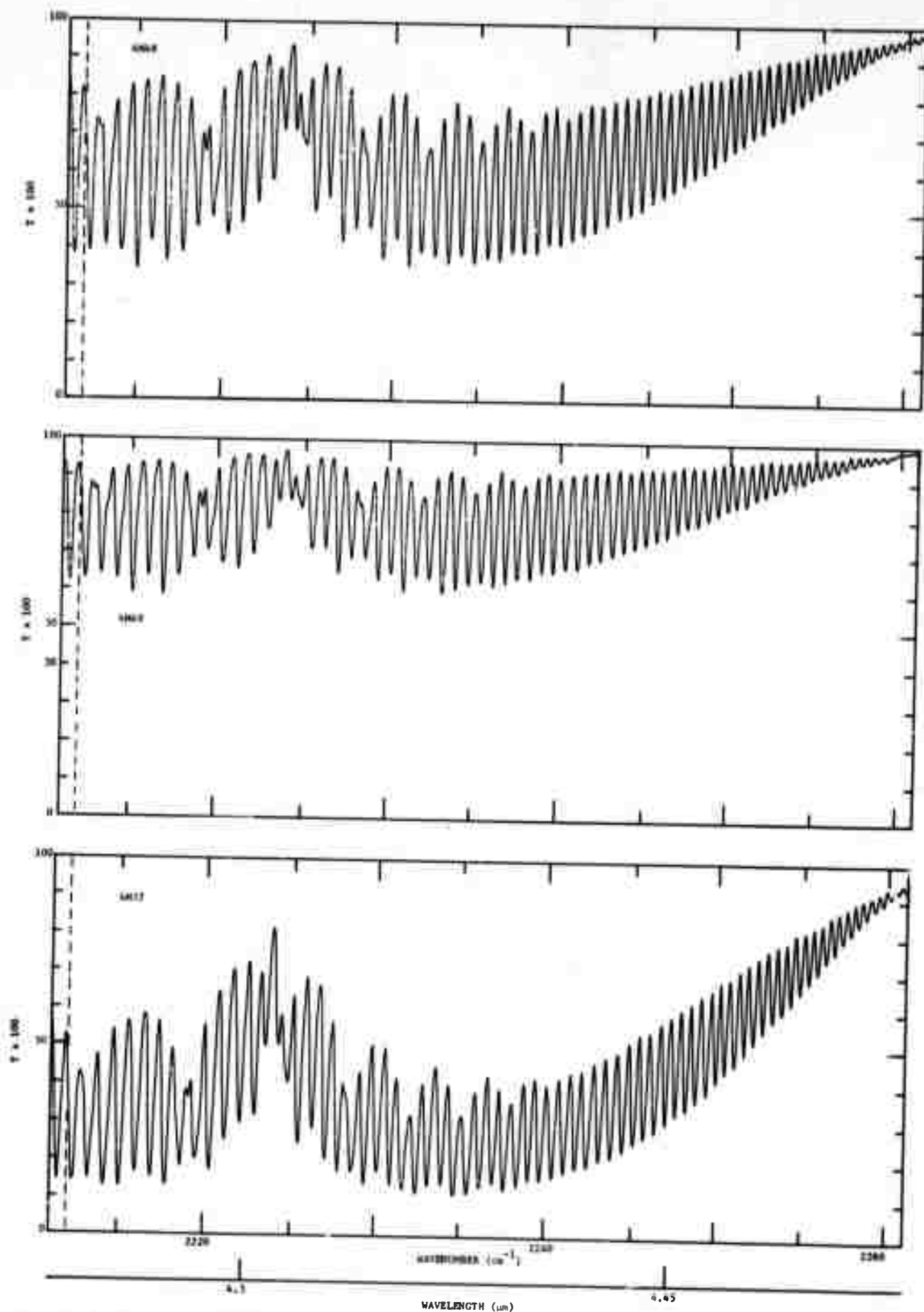


FIG. 4-4. Spectral curves of transmittance between 2210 and 2260  $cm^{-1}$ . The sample parameters are given in Table 4-1. Spectral slitwidth = 0.3  $cm^{-1}$ .

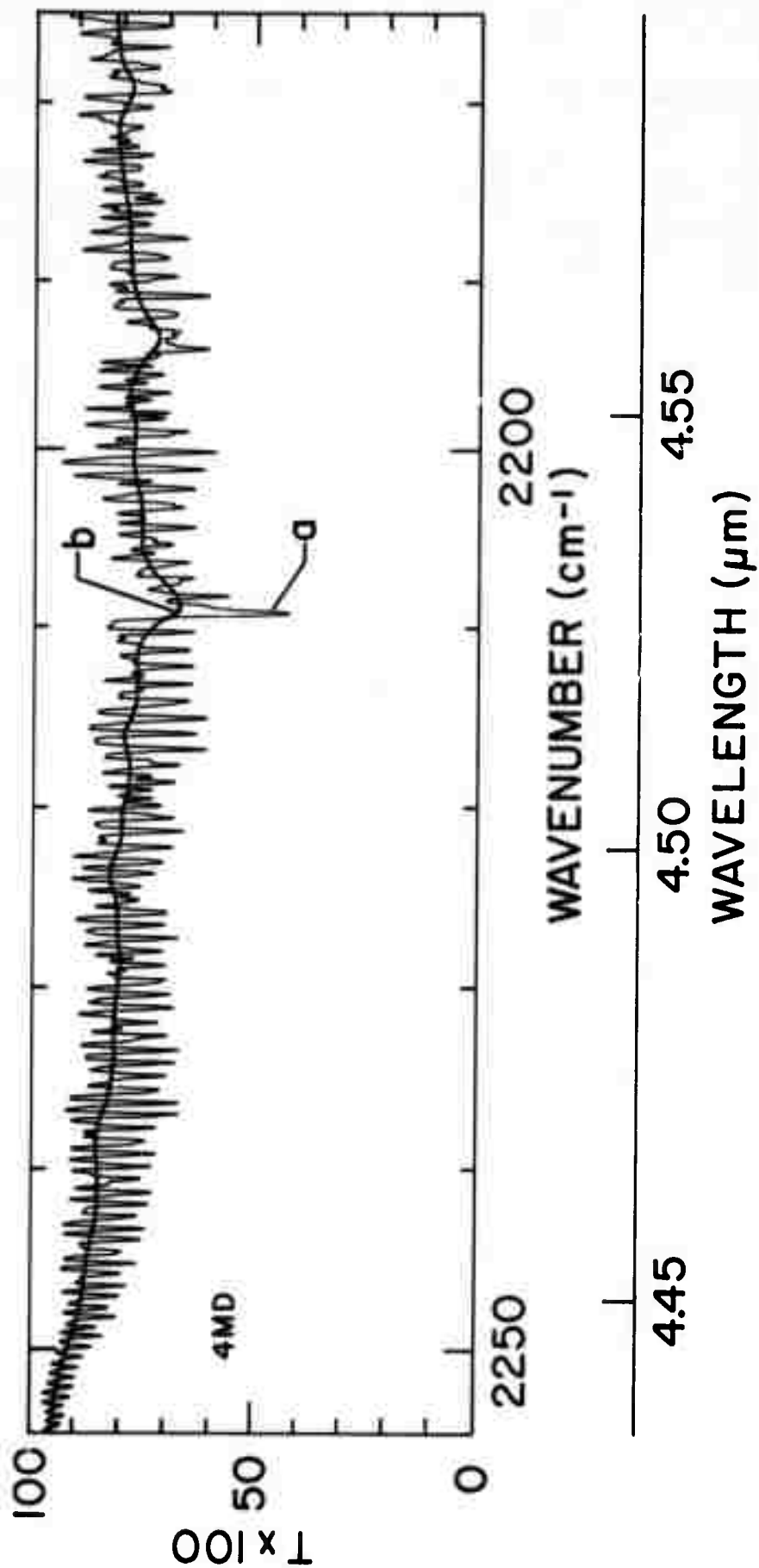


FIG. 4-5. Spectral curves of transmittance for a sample at  $0.97 \times 10^{-4}$  atm. Both curves represent the same sample of pure  $\text{H}_2\text{O}$ . Spectral slitwidth  $\approx 0.2 \text{ cm}^{-1}$  for curve a and  $2.2 \text{ cm}^{-1}$  for curve b.

## SECTION 5

### REFERENCES

1. L. D. Gray Young, J. Quant. Spectrosc. Radiative Transfer (1971).
2. D. F. Eggers and B. L. Crawford, J. Chem. Phys. 19, 1554 (1951).
3. D. E. Burch, D. A. Gryvnak, and R. R. Patty, J. Opt. Soc. Am. 57, 885 (1967).
4. Josef Pliva, J. Mol. Spectry. 25, 62 (1968).
5. Josef Pliva, J. Mol. Spectry. 27, 461 (1968).
6. R. M. Goody and T. W. Wormell, Proc. Roy. Soc. A209, 178 (1951).
7. D. E. Burch, D. A. Gryvnak, R. R. Patty, and C. E. Bartky, J. Opt. Soc. Am. 59, 267 (1969); also  
D. E. Burch, D. A. Gryvnak, R. R. Patty, and C. E. Bartky, "The Shapes of Collision-broadened CO<sub>2</sub> Lines", Contract Number NONr 3560(00), Aeronutronic Publication Number U-3203, 31 August 1968.